Research Paper
Computational Methods for Differential Equations
http://cmde.tabrizu.ac.ir
Vol. *, No. *, *, pp. 1-31
DOI:10.22034/cmde.2026.70617.3519

High-order numerical solutions for dynamic equations on time scales: Theory, implementation, and applications

Khalid K. Ali[1,2,*], **Kamal R. Raslan**[1], **Mohamed S. Mohamed**[3], **and Ahmed Azaba**[4]

[1]Department of Mathematics, Faculty of Science, Al-Azhar University, Nasr-City, Cairo, Egypt.

[2]Mathematics Education Program, Faculty of Education and Arts, Sohar University, Sohar 311, Oman.

[3]Department of Mathematics, College of Science, Taif University, P.O. Box 11099, Taif, 21944, Saudi Arabia.

[4]Al-Ryada University for Science and Technology, Sadat City, Menoufia, Egypt.

Abstract

In this paper, we introduce a numerical method for solving dynamic equations on time scales, using the two-stage of the Runge-Kutta method. Time-scale calculus offers a unified framework that brings together continuous and discrete analysis, making it well-suited for modeling systems that evolve in both smooth and stepwise manners, as commonly encountered in biology, engineering, economics, and control theory. Our approach adapts the classical Runge-Kutta method to the unique features of time scale calculus, incorporating key elements such as the delta derivative, graininess function, and the forward jump operator. The method is designed to maintain second-order accuracy while working efficiently across various time domains, whether they are densely packed or contain scattered points, without requiring a switch between separate discrete and continuous models. We further demonstrate that, when specialized to $\mathbb{T} = \mathbb{R}$, the proposed method reduces exactly to the classical second-order Runge-Kutta method, confirming that the time-scale framework is a proper generalization of the continuous case. To test the method's effectiveness, we apply it to a variety of example problems, including both linear and nonlinear dynamic equations. These examples include functions of exponential, trigonometric, and rational forms. In each case, we compare our numerical results to known exact solutions, using plots and error analysis to assess performance. The results consistently demonstrate strong accuracy across diverse scenarios. A convergence study confirms the theoretical second-order rate $p \approx 2.00$ at every refinement level, and a stability test under perturbed initial data shows that the relative error remains bounded by the size of the perturbation throughout the domain.

Keywords. Time scale, Dynamic equation, Numerical solution, Exact solution, Runge-Kutta method.

2010 Mathematics Subject Classification. 65L05, 34K06, 34K28.

Uncorrected Proof

1. Introduction

A time-scale $\mathbb{T}$ is a nonempty closed subset of the real numbers [2]. It may consist of isolated points (to modeling discrete events), continuous intervals (for ongoing processes), or a mix of both [2]. For example, setting $\mathbb{T} = \mathbb{R}$ recovers classical differential calculus, while $\mathbb{T} = \mathbb{Z}$ gives us standard difference equations [2]. One of the main ideas in the theory is the *delta derivative*, which extends the concept of a derivative to this combined domain, enabling smooth transitions between discrete and continuous analyses [24]. The concept of time scales, which has recently attracted significant interest, unifies both the continuous and discrete behaviors. It was introduced by Stefan Hilger in his doctoral dissertation to unify discrete and continuous analysis [23]. The fundamental idea is to establish results for a dynamic equation where the domain of the unknown function is referred to as a time scale T, which may represent any closed subset of the real numbers $\mathbb{R}$ [24]. The three most notable instances of calculus on time scales are differential calculus, difference calculus, and quantum calculus with $\mathbb{T} = \mathbb{R}$ and $\mathbb{T} = \mathbb{Z}$,$\mathbb{T} = \overline{q^{\mathbb{Z}}} = \{q^z : z \in \mathbb{Z}\} \cup \{0\}$ where $q > 1$ [2]. The book by Bohner and Peterson compiles and organizes much of the calculus on time scales [10]. All

Received: *; Accepted:*.

∗ Corresponding author. Email: khalidkaram2012@azhar.edu.eg.

notations related to time scales are defined in the following section. Since its introduction, the theory has significantly evolved [2]. Building upon Hilger's foundational research, scholars like Aulbach and Bohner have broadened its reach, while others such as Atici and Uysal have advanced its applications, particularly in simulating real-world systems [6, 7]. On the theoretical side, Bohner and Georgiev expanded the paradigm to multivariable dynamic calculus [14], and the overarching mathematical objective of uniting differential and difference calculus has been substantially realized [25]. Apart from foundational calculus operations, theoretical research has largely concentrated on defining fundamental features of dynamic equations. This involves establishing the boundedness and uniqueness of solutions [29, 31], constructing new dynamic inequalities [28], and solving complex boundary value problems utilizing Green's functions and variational techniques [3, 4, 33]. Additionally, significant study has been committed to assessing the stability and instability of both time-varying linear and nonlinear dynamic systems on time scales [17, 26, 29]. Time-scale theory has found deep application in the basic sciences. In biology and ecology, time scale calculus is used to represent dynamic processes with time domains that are mixed between integers (difference equations) or real numbers (differential equations) [12, 13]. For example, time scale calculus is frequently employed to model insect populations that are sometimes continuous and at other times discrete, following a fixed step size [13, 34]. Economics is a particularly suitable domain for applying time scale methods[5]. Dynamic economic models are established in either continuous or discrete time frames [5]. In a discrete model, for instance, a consumer obtains income during a specific time period and then decides how much to save and consume within that same period [5]. This means that all decisions are presumed to be made at regular intervals. Applying time scale calculus to this optimization problem is considerably more adaptable and realistic [5, 21]. For instance, a consumer may receive income at one moment, adjust their asset holdings at another moment, and consume at yet another time [5]. Time scale theory has also gained significant importance in engineering. Many systems integrate continuous dynamics such as heat transfer or fluid movement with discrete elements like switches, relays, or sensor activation [9]. By using a hybrid time scale such as $\mathbb{T} = [0, 1] \cup \{2, 3, 4\}$, engineers are able to capture both steady state behaviors and abrupt changes within a unified model [9]. In physics, this theory establishes a novel geometric framework where scaling laws work alongside laws of motion[1]. This perspective begins with the observation that modern physics rests on the debatable assumption of a smooth spacetime continuum [1]. Although this premise seems to hold in classical physics, it is clearly contradicted by phenomena observed in quantum mechanics [18]. In fact, Feynman showed that the typical paths of quantum particles are a hybrid of continuous and discrete [18]. Time scale theory extends beyond the basic sciences to engineering applications including control theory, environmental monitoring, and epidemiology [9, 13]. This includes modeling control systems that alternate between continuous and discrete states, monitoring environmental shifts that feature both gradual trends and sudden changes [9]. We can also use it in examining disease dynamics influenced by both steady transmission and seasonal increases[13]. Time-scale calculus provides a reliable and adaptable method for real-world dynamic applications [2].

While time scale calculus is an excellent tool for modeling hybrid dynamic systems, finding exact analytical solutions is rarely possible in practice. This creates a strong need for reliable numerical methods. However, standard discretization techniques often lose accuracy or become computationally expensive when applied to scattered time domains. To overcome this, we propose a two-stage Runge-Kutta method adapted specifically for time scale calculus. By integrating the delta derivative, the graininess function, and the forward jump operator, our approach avoids the need to switch between continuous and discrete models. Ultimately, this yields a stable, second-order-accurate tool that can be readily applied to simulate complex systems across any arbitrary time domain.

This paper is organized as follows: Section 2 introduces the preliminaries of time scale calculus, including key operators, derivatives, and integration. Section 3 presents the formulation of dynamic equations on time scales and the adaptation of the Runge-Kutta method for such systems. Section 4 provides new theoretical results, including consistency and accuracy analysis of the proposed method. Section 5 demonstrates the method's effectiveness through numerical examples, comparing results with exact solutions. Section 6 concludes the paper with a summary of findings and potential future directions.

Uncorrected Proof

2. Preliminaries

2.1. **Time Scale Calculus.** We use the symbol $\mathbb{T}$ to denote a time scale. We assume that a time scale $\mathbb{T}$ possesses a topology derived from the real numbers with the standard topology, and such structures are often analyzed within the broader context of dynamic systems on measure chains [10, 27]. The following definitions and operators are key concepts in time-scale calculus [10].

2.2. **Forward and Backward Jump Operators.**

- **Forward Jump Operator** $\sigma : \mathbb{T} \to \mathbb{T}$, is defined as [10, 14]:

  $\sigma(\psi) = \inf\{s \in \mathbb{T} : s > \psi\}$.

- **Backward Jump Operator** $\rho : \mathbb{T} \to \mathbb{T}$, is defined as [10, 14]:

  $\rho(\psi) = \sup\{s \in \mathbb{T} : s < \psi\}$.

2.3. **Graininess Functions.**

- **Forward Graininess Function** $\mu : \mathbb{T} \to \mathbb{R}$, is defined as [10]:

  $\mu(\psi) = \sigma(\psi) - \psi$.

- **Backward Graininess Function** $\nu : \mathbb{T} \to \mathbb{R}$, is defined as [10]:

  $\nu(\psi) = \psi - \rho(\psi)$.

2.4. **Derivatives on Time Scales.**

Delta Derivative. Assume that $\Xi : \mathbb{T} \to \mathbb{R}$, is a function and let $\psi \in \mathbb{T}^\kappa$. We define $\Xi^\Delta(\psi)$ to be the number, provided it exists, with the property that for any $\varepsilon > 0$, there exists a neighbourhood U of ψ, $U = (\psi - \delta, \psi + \delta) \cap \mathbb{T}$, for some $\delta > 0$, such that

$$|\Xi(\sigma(\psi)) - \Xi(s) - \Xi^\Delta(\psi)(\sigma(\psi) - s)| \leq \varepsilon|\sigma(\psi) - s| \quad \text{for all } s \in U,$$

see [10, 24].

We call $\Xi^\Delta(\psi)$ the *delta* or *Hilger* derivative of Ξ at ψ, shortly *differentiable* [10, 14], in $\mathbb{T}^\kappa$ if $\Xi^\Delta(\psi)$ exists for all $\psi \in \mathbb{T}^\kappa$. The function $\Xi^\Delta : \mathbb{T} \to \mathbb{R}$, is said to be the *delta derivative* or *Hilger derivative*, shortly *derivative*, of Ξ in $\mathbb{T}^\kappa$.

Note that if $\mathbb{T} = \mathbb{R}$, then the delta derivative coincides with the classical derivative.

Nabla Derivative. Let $\Xi : \mathbb{T} \to \mathbb{R}$. The **nabla derivative** $\Xi^\nabla(\psi)$ at a point $\psi \in \mathbb{T}$ is defined by:

$$\forall \varepsilon > 0, \quad \exists \delta_\varepsilon > 0 \quad \text{such that} \quad \forall s \in \mathbb{T}, \quad |s - \psi| < \delta_\varepsilon \Rightarrow \left|\Xi(\rho(\psi)) - \Xi(s) - \Xi^\nabla(\psi)(\psi - s)\right| \leq \varepsilon|\psi - s|.$$

If such a value does not exist, Ξ is **not nabla differentiable** at ψ, [11].

2.5. **Theorems on Derivatives.**

Delta Derivative Theorem. Let $\Xi : \mathbb{T} \to \mathbb{R}$, be continuous, and $\psi \in \mathbb{T}^\kappa$. Then, [10]:

- If ψ is **right-dense**:

  $$\Xi^\Delta(\psi) = \lim_{s \to \psi} \frac{\Xi(\psi) - \Xi(s)}{\psi - s} = \Xi'(\psi).$$

- If ψ is **right-scattered**:

  $$\Xi^\Delta(\psi) = \frac{\Xi(\sigma(\psi)) - \Xi(\psi)}{\sigma(\psi) - \psi}.$$

Uncorrected Proof

2.6. **Integration on Time Scales.**

Definition 2.1. A function $f : \mathbb{T} \to \mathbb{R}$, is called *regulated* provided its right-sided limits exist (finite) at all right-dense points in $\mathbb{T}$ and its left-sided limits exist (finite) at all left-dense points in $\mathbb{T}$ [32].

Definition 2.2. A continuous function $f : \mathbb{T} \to \mathbb{R}$, is called *pre-differentiable* [20] with (region of differentiation) D, provided

(1) $D \subset \mathbb{T}^{\kappa}$,
(2) $\mathbb{T}^{\kappa} \setminus D$ is countable and contains no right-scattered elements of $\mathbb{T}$,
(3) f is differentiable at each $\psi \in D$.

The **delta integral** is defined as [20]:

$$\int \Xi(\psi)\Delta\psi = F(\psi) + C,$$

where Ξ is pre-differentiable. The Cauchy integral is then:

$$\int_r^s \Xi(\psi)\Delta\psi = F(s) - F(r), \quad \forall r, s \in \mathbb{T}.$$

2.7. **rd-Continuous and Regressive Functions.** To accurately define exponential functions and solve linear dynamic equations on time scales, we must classify specific types of functions.

Definition 2.3. rd-Continuous: A function $\Xi : \mathbb{T} \to \mathbb{R}$, is said to be *rd-continuous* if it is continuous at all right-dense points in $\mathbb{T}$ and its left-sided limits exist (and are finite) at all left-dense points in $\mathbb{T}$. The set of all rd-continuous functions is denoted by $C_{rd} = C_{rd}(\mathbb{T}, \mathbb{R})$ [10, 11, 24].

Definition 2.4. Regressive: An rd-continuous function $p : \mathbb{T} \to \mathbb{R}$ is called *regressive* if it satisfies the condition:

$$1 + \mu(\psi)p(\psi) \neq 0 \quad \text{for all } \psi \in \mathbb{T}^{\kappa}.$$

The set of all rd-continuous and regressive functions is denoted by $\mathcal{R}$ [10, 11, 24].

2.8. **Exponential and Trigonometric Functions on Time Scales.**

- **Exponential Function** [10]: For $p \in \mathcal{R}$, the exponential function on time scales $\mathbb{T}$ is defined as:

$$e_p(\psi, s) = \exp\left(\int_s^{\psi} \xi_{\mu(\tau)}(p(\tau))\Delta\tau\right), \quad \text{for } \psi, s \in \mathbb{T},$$

where the cylinder transformation $\xi_h(z)$ is given by:

$$\xi_h(z) = \begin{cases} \frac{\mathrm{Log}(1+hz)}{h}, & h \neq 0, \\ z, & h = 0. \end{cases}$$

- **Trigonometric Functions** [10]: If $\Xi \in C_{rd}$, the time scale sine and cosine functions are defined by:

$$\cos_{\Xi} = \frac{e_{if} + e_{-if}}{2}, \quad \sin_{\Xi} = \frac{e_{if} - e_{-if}}{2i}.$$

Table 1 and Table 2 present the explicit forms of the exponential and trigonometric functions on selected time scales [10]. For both tables, we define $i = \sqrt{-1}$.

Uncorrected Proof

TABLE 1. Time scale exponential functions.

Time Scale	Expression
$\mathbb{T}$	$e_\alpha(\psi,\psi_0)$
$\mathbb{R}$	$e^{\alpha(\psi-\psi_0)}$
$\mathbb{Z}$	$(1+\alpha)^{\psi-\psi_0}$
$h\mathbb{Z}$	$(1+\alpha h)^{(\psi-\psi_0)/h}$
$\frac{1}{n}\mathbb{Z}$	$\left(1+\frac{\alpha}{n}\right)^{n(\psi-\psi_0)}$
$q^{\mathbb{N}_0}$	$\prod_{s\in[\psi_0,\psi)}[1+(q-1)\alpha s]$ if $\psi>\psi_0$
$2^{\mathbb{N}_0}$	$\prod_{s\in[\psi_0,\psi)}(1+\alpha s)$ if $\psi>\psi_0$

TABLE 2. Trigonometric functions on time scales.

Time Scale ($\mathbb{T}$)	Cosine Function $\cos_\alpha(\psi,\psi_0)$	Sine Function $\sin_\alpha(\psi,\psi_0)$
$\mathbb{R}$	$\cos(\alpha(\psi-\psi_0))$	$\sin(\alpha(\psi-\psi_0))$
$\mathbb{Z}$	$\frac{(1+i\alpha)^{\psi-\psi_0}+(1-i\alpha)^{\psi-\psi_0}}{2}$	$\frac{(1+i\alpha)^{\psi-\psi_0}-(1-i\alpha)^{\psi-\psi_0}}{2i}$
$h\mathbb{Z}$	$\frac{(1+ih\alpha)^{(\psi-\psi_0)/h}+(1-ih\alpha)^{(\psi-\psi_0)/h}}{2}$	$\frac{(1+ih\alpha)^{(\psi-\psi_0)/h}-(1-ih\alpha)^{(\psi-\psi_0)/h}}{2i}$
$q^{\mathbb{N}_0}$	$\prod_{k=\psi_0}^{\psi-1}\left(1+\frac{(q-1)\alpha^2k^2}{2}\right)\left(1+(q-1)^2\alpha^2k^2\right)^{-1}$	$\alpha\prod_{k=\psi_0}^{\psi-1}\frac{(2q-1)k}{1+(q-1)^2\alpha^2k^2}$

Uncorrected Proof

2.9. Time Scale Monomials.

Definition 2.5. Let $s,\psi\in\mathbb{T}$. The *time scale monomials* are defined recursively by [10]

$$g_0(\psi,s)=h_0(\psi,s)=1,$$

and for $k\in\mathbb{N}_0$,

$$g_{k+1}(\psi,s)=\int_s^\psi g_k(\sigma(\tau),s)\Delta\tau,\quad h_{k+1}(\psi,s)=\int_s^\psi h_k(\tau,s)\Delta\tau.$$

Remark 2.6. We compute the first few monomials [10]:

$$g_1(\psi,s)=\int_s^\psi g_0(\sigma(\tau),s)\Delta\tau=\int_s^\psi 1\,\Delta\tau=\psi-s,$$
$$h_1(\psi,s)=\int_s^\psi h_0(\tau,s)\Delta\tau=\int_s^\psi 1\,\Delta\tau=\psi-s,$$
$$g_2(\psi,s)=\int_s^\psi g_1(\sigma(\tau),s)\Delta\tau=\int_s^\psi(\sigma(\tau)-s)\Delta\tau,$$
$$h_2(\psi,s)=\int_s^\psi h_1(\tau,s)\Delta\tau=\int_s^\psi(\tau-s)\Delta\tau.$$

Moreover, the delta derivatives satisfy

$$g_k^\Delta(\psi,s)=g_{k-1}(\sigma(\psi),s),\quad h_k^\Delta(\psi,s)=h_{k-1}(\psi,s),\quad k\in\mathbb{N}.$$

Theorem 2.7 (Taylor's Formula). *[10] Let $n\in\mathbb{N}$. Suppose Ξ is n times delta differentiable on $\mathbb{T}^{\kappa^n}$. Let $\alpha\in\mathbb{T}^{\kappa^{n-1}}$ and $\psi\in\mathbb{T}$. Then*

$$\Xi(\psi)=\sum_{k=0}^{n-1}h_k(\psi,\alpha)\Xi^{\Delta^k}(\alpha)+\int_\alpha^{\rho^{n-1}(\psi)}h_{n-1}(\psi,\sigma(\tau))\Xi^{\Delta^n}(\tau)\Delta\tau.$$

Suppose that $r > 0$, $\psi, \psi + r \in [\psi_0, \psi_f]$, $\rho^2(\psi + r) \in [\psi_0, \psi_f]$. Then, by the Taylor formula of the second-order [10, 19], we compute

$$\Upsilon(\psi + r) = \Upsilon(\psi) + h_1(\psi + r, \psi)\Upsilon^{\Delta}(\psi) + h_2(\psi + r, \psi)\Upsilon^{\Delta^2}(\psi) + \int_{\psi}^{\psi+r} h_2(\psi + r, \sigma(\tau))\Upsilon^{\Delta^3}(\tau)\Delta\tau.$$

Let

$$R_2(r) = \int_{\psi}^{\psi+r} h_2(\psi + r, \sigma(\tau))\Upsilon^{\Delta^3}(\tau)\Delta\tau.$$

Then

$$\Upsilon(\psi + r) = \Upsilon(\psi) + h_1(\psi + r, \psi)\Upsilon^{\Delta}(\psi) + h_2(\psi + r, \psi)\Upsilon^{\Delta^2}(\psi) + R_2(r).$$

2.10. **Finite Difference Operators.**

Definition 2.8 (First-Order Finite Difference Operator Δ_1)**.** [19] The first-order finite difference operator, denoted as Δ_1, provides an explicit finite difference approximation of the delta derivative and is defined as:

$$\Delta_1\Xi(\psi) = \frac{\Xi(\sigma(\psi)) - \Xi(\psi)}{\sigma(\psi) - \psi}, \quad \psi \in \mathbb{T}.$$

- In the continuous case ($\mathbb{T} = \mathbb{R}$), as $\sigma(\psi) \to \psi$, we obtain $\Delta_1\Xi(\psi) \to \Delta\Xi(\psi) = \Xi'(\psi)$ [19].
- In the discrete case ($\mathbb{T} = \mathbb{Z}$), we recover the standard forward difference:

$$\Delta_1\Xi(\psi) = \Xi(\psi + 1) - \Xi(\psi).$$

Definition 2.9 (Second-Order Finite Difference Operator Δ_2)**.** [19] The second-order finite difference operator, denoted as $\Delta_2\Xi(\psi)$, measures how the first-order finite difference $\Delta_1\Xi(\psi)$ changes over time. It is defined as:

$$\Delta_2\Xi(\psi) = \Delta_1(\Delta_1\Xi(\psi)),$$

Expanding using the definition of Δ_1:

$$\Delta_2\Xi(\psi) = \frac{\Delta_1\Xi(\sigma(\psi)) - \Delta_1\Xi(\psi)}{\sigma(\psi) - \psi}.$$

For an arbitrary time scale $\mathbb{T}$, using the delta operator:

$$\Delta_2\Xi(\psi) = \frac{\Xi(\sigma^2(\psi)) - \Xi(\sigma(\psi))}{\sigma(\psi) - \psi} - \frac{\Xi(\sigma(\psi)) - \Xi(\psi)}{\sigma(\psi) - \psi}.$$

This expression captures second-order changes in a function on time scales.

TABLE 3. Comparison between the Delta operator and the first-order finite difference.

Feature	Δ **(Delta Operator)**	Δ_1 **(First-Order Finite Difference)**
Definition	$\lim_{\sigma(\psi)\to\psi} \frac{\Xi(\sigma(\psi)) - \Xi(\psi)}{\sigma(\psi) - \psi}$	$\frac{\Xi(\sigma(\psi)) - \Xi(\psi)}{\sigma(\psi) - \psi}$
Type	General differentiation operator on time scales	Explicit finite difference approximation
Continuous Case ($\mathbb{T} = \mathbb{R}$)	$\Delta\Xi(\psi) = \Xi'(\psi)$	$\Delta_1\Xi(\psi) \approx \Xi'(\psi)$
Discrete Case ($\mathbb{T} = \mathbb{Z}$)	$\Delta\Xi(\psi) = \Xi(\psi + 1) - \Xi(\psi)$	$\Delta_1\Xi(\psi) = \Xi(\psi + 1) - \Xi(\psi)$
Limit Process	Involves a limit process	No limit is taken
Use in Calculus	Defines smooth differentiation on time scales	Used for numerical and discrete approximations

Uncorrected Proof

2.11. **Comparison Table: Δ vs. Δ_1.** In Section 4, we formulate the dynamic equations based on these operators.

3. Dynamic equation on Time Scales

Theorem 3.1 (Variation of Constants)**.** *[10] Suppose $p \in \mathbb{R}$ and $\Xi \in C_{rd}$. Let $\psi_0 \in \mathbb{T}$ and $y_0 \in \mathbb{R}$. The unique solution of the initial value problem*

$$\mathcal{Y}^{\Delta} = p(\psi)\mathcal{Y} + \Xi(\psi), \quad \mathcal{Y}(\psi_0) = y_0,$$

is given by

$$\mathcal{Y}(\psi) = e_p(\psi, \psi_0)y_0 + \int_{\psi_0}^{\psi} e_p(\psi, \sigma(\tau))\Xi(\tau)\,\Delta\tau.$$

Definition 3.2 (Two-Stage Runge-Kutta Method)**.** [15, 30] Under hypotheses (H1) and (H2), let $\psi_{n+1}^1 = \psi_n + r_{n+1}^1 \in \mathbb{T}$ with $\psi_n < \psi_n + r_{n+1}^1 < \psi_n + r_{n+1}$. The two-stage Runge-Kutta method is defined by:

$$\begin{aligned} k_1 &= \Xi(\psi_n, \Upsilon_n), \\ k_2 &= a_1\Xi(\psi_{n+1}^1, \Upsilon_n) + a_2\Xi\left(\psi_n, \Upsilon_n + \frac{h_2(\psi_{n+1}^1, \psi_n)g(\psi_n, \Upsilon_n)}{\Xi_\Upsilon(\psi_n, \Upsilon_n)} r_{n+1}^1\right), \\ \Upsilon_{n+1} &= \Upsilon_n + r_{n+1}^1(b_1k_1 + b_2k_2), \end{aligned}$$

where:

(H1):

$$\begin{cases} |\Xi(\psi, \Upsilon)| \le A, & \psi \in \mathbb{T},\ \Upsilon \in \mathbb{R}, \\ \text{there exist } \Delta_1\Xi(\psi, \Upsilon) \text{ and } \dfrac{\partial}{\partial \Upsilon}\Xi(\psi, \Upsilon) \text{ such that} & \\ |\Delta_1\Xi(\psi, \Upsilon)| \le A, \quad \left|\dfrac{\partial}{\partial \Upsilon}\Xi(\psi, \Upsilon)\right| \le A, & \psi \in \mathbb{T},\ \Upsilon \in \mathbb{R}, \end{cases}$$

for some positive constant A.

(H2):

$$\frac{\partial \Xi}{\partial \Upsilon}(\psi, \Upsilon) \neq 0, \qquad (\psi, \Upsilon) \in [a, b] \times \mathbb{R}.$$

- $a_1, a_2, b_1, b_2 \in \mathbb{R}$ are coefficients.
- k_1, k_2 are the stage approximations.
- Δ_1 denotes the first-order finite difference operator.
- h_2 is a time scale monomial function.
- $g(\psi_n, \Upsilon_n)$ captures additional dynamics.

Consistency Conditions:

- For first-order accuracy ($p = 1$):

$$\begin{cases} b_1 + b_2(a_1 + a_2) = 1, \\ a_1b_2 \neq 0. \end{cases} \quad \text{or} \quad \begin{cases} b_1 + b_2(a_1 + a_2) = 1, \\ a_2b_2 \neq 1. \end{cases}$$

- For second-order accuracy ($p = 2$):

$$\begin{cases} b_1 + b_2(a_1 + a_2) = 1, \\ a_1b_2 = 0, \\ a_2b_2 = 1. \end{cases}$$

Uncorrected Proof

Definition 3.3 (s-Stage Runge-Kutta Method)**.** [16, 19, 30] Under hypotheses (H1) and (H2), with $\psi_{n+1}^1 = \psi_n + r_{n+1}^1 \in \mathbb{T}$ such that $\psi_n < \psi_n + r_{n+1}^1 < \psi_n + r_{n+1}$, the general $s$stage Runge-Kutta method is defined as:

$$\Upsilon_{n+1} = \Upsilon_n + r_{n+1}^1 \sum_{j=1}^{s} b_j k_j,$$

where the stage values k_j are given by:

$$\begin{aligned} k_1 &= \Xi(\psi_n, \Upsilon_n), \\ k_j &= k_j(\Xi, \Delta_1 \Xi, \Xi_\Upsilon), \quad \text{for } j = 2, \ldots, s. \end{aligned}$$

The coefficients b_j are determined by expanding Ξ, Υ, and k_j in Taylor series up to order $p > 0$, ensuring consistency of order p.

4. Some New Elementary Results

Theorem 4.1. *Consider the initial value problem (IVP) on a time scale* $\mathbb{T}$

$$\begin{cases} \Upsilon^{\Delta}(\psi) = \Xi(\psi, \Upsilon(\psi)), & \psi \in [a, b] \subset \mathbb{T}, \\ \Upsilon(\psi_0) = \Upsilon_0, & \Upsilon_0 \in \mathbb{R}, \end{cases}$$

where $\Xi : [a, b] \times \mathbb{R} \to \mathbb{R}$ *satisfies:*

(H1) *There exists* $A > 0$ *such that* $|\Xi(\psi, \Upsilon)| \leq A$, $|\Delta_1 \Xi(\psi, \Upsilon)| \leq A$, *and* $|\Xi_\Upsilon(\psi, \Upsilon)| \leq A$ *for all* $\psi \in \mathbb{T}$, $\Upsilon \in \mathbb{R}$.
(H2) $\frac{\partial \Xi}{\partial \Upsilon}(\psi, \Upsilon) \neq 0$ *for all* $(\psi, \Upsilon) \in [a, b] \times \mathbb{R}$.

For a sequence of time points $\{\psi_n\}$ *in* $[a, b]$ *with intermediate steps* $\psi_{n+1}^1 = \psi_n + r_{n+1}^1$, $\psi_{n+1} = \psi_n + r_{n+1}$, *where* $\psi_n < \psi_{n+1}^1 < \psi_{n+1}$, *the two-stage method*

$$\begin{aligned} \Upsilon_n &= \Upsilon(\psi_n), \\ \Upsilon_{n+1} &= \Upsilon_n + r_{n+1}^1 (b_1 k_1 + b_2 k_2), \\ k_1 &= \Xi(\psi_n, \Upsilon_n), \\ k_2 &= a_1 \Xi(\psi_{n+1}^1, \Upsilon_n) + a_2 \Xi\left(\psi_n, \Upsilon_n + \frac{h_2(\psi_{n+1}^1, \psi_n)}{r_{n+1}^1} \cdot \frac{g(\psi_n, \Upsilon_n)}{\Xi_\Upsilon(\psi_n, \Upsilon_n)}\right), \end{aligned}$$

with constants $a_1, a_2, b_1, b_2 \in \mathbb{R}$ *and smooth functions* g, h_2, *is consistent and achieves second-order accuracy.*

When $\mathbb{T} = \mathbb{R}$, *the IVP becomes*

$$\frac{d\Upsilon}{d\psi} = \Xi(\psi, \Upsilon(\psi)), \quad \Upsilon(\psi_0) = \Upsilon_0,$$

and the method reduces to the classical second-order Runge-Kutta method

$$\begin{aligned} \Upsilon_{i+1} &= \Upsilon_i + r(a_1 k_1 + a_2 k_2), \\ k_1 &= \Xi(\psi_i, \Upsilon_i), \\ k_2 &= \Xi(\psi_i + p_1 r, \Upsilon_i + q_{11} k_1 r), \end{aligned}$$

with step size r *and coefficients* $a_1, a_2, p_1, q_{11} \in \mathbb{R}$, *achieving second-order accuracy under conditions (H1), (H2), and standard Butcher conditions.*

Uncorrected Proof

Proof. To establish the foundation for our result, we first recall the general derivation on a time scale $\mathbb{T}$ as presented in [19]. Following their methodology, we start with the Taylor expansion:

$$\begin{aligned}
\Upsilon(\psi_{n+1}) &= \Upsilon(\psi_n + r^1_{n+1}\psi_n) \\
&= \Upsilon(\psi_n) + r^1_{n+1}\Delta_1\psi_n + h_2(\psi_{n+1},\psi_n)g(\psi_n,\Upsilon_n) + \mathcal{O}(r^3) \\
&= \Upsilon_n + r^1_{n+1}\Xi(\psi_n,\Upsilon_n) + h_2(\psi_{n+1},\psi_n)g(\psi_n,\Upsilon_n) + \mathcal{O}(r^3), \\
\Xi(\psi_{n+1},\Upsilon_n) &= \Xi(\psi_n,\Upsilon_n) + r^1_{n+1}\Delta_1\Xi(\psi_n,\Upsilon_n) + \mathcal{O}(r^2), \\
\Xi\left(\psi_n,\Upsilon_n + \frac{h_2(\psi_{n+1},\psi_n)}{r^1_{n+1}}\cdot\frac{g(\psi_n,\Upsilon_n)}{\Xi_\Upsilon(\psi_n,\Upsilon_n)}\right) &= \Xi(\psi_n,\Upsilon_n) + \frac{h_2(\psi_{n+1},\psi_n)}{r^1_{n+1}}\cdot\frac{g(\psi_n,\Upsilon_n)}{\Xi_\Upsilon(\psi_n,\Upsilon_n)}\Xi_\Upsilon(\psi_n,\Upsilon_n) + \mathcal{O}(r^2) \\
&= \Xi(\psi_n,\Upsilon_n) + g(\psi_n,\Upsilon_n)\frac{h_2(\psi_{n+1},\psi_n)}{r^1_{n+1}} + \mathcal{O}(r^2).
\end{aligned}$$

We call:

$$g(\psi,\Upsilon(\psi)) = \Upsilon^{\Delta^2}(\psi)$$

Then,

$$g(\psi,\Upsilon(\psi)) = \Delta_1\Xi(\psi,\Upsilon(\psi)) + \left(\int_0^1 \frac{\partial}{\partial\Upsilon}\Xi\big(\sigma(\psi),\Upsilon(\psi) + s\mu(\psi)\Xi(\psi,\Upsilon(\psi))\big)ds\right)\Xi(\psi,\Upsilon(\psi)).$$

We define:

$$\begin{aligned}
k_2 &= a_1\Xi(\psi_{n+1},\Upsilon_n) + a_2\Xi\left(\psi_n,\Upsilon_n + \frac{h_2(\psi_{n+1},\psi_n)}{r_{n+1}}\cdot\frac{g(\psi_n,\Upsilon_n)}{\Xi_\Upsilon(\psi_n,\Upsilon_n)}\right) \\
&= a_1(\Xi(\psi_n,\Upsilon_n) + r^{n+1}_{n+1}\Delta_1\Xi(\psi_n,\Upsilon_n) + \mathcal{O}(r^2) \\
&+ a_2\left(\Xi(\psi_n,\Upsilon_n) + g(\psi_n,\Upsilon_n)\frac{h_2(\psi_{n+1},\psi_n)}{r_{n+1}} + \mathcal{O}(r^2)\right) \\
&= (a_1+a_2)\Xi(\psi_n,\Upsilon_n) + a_1r^1_{n+1}\Delta_1\Xi(\psi_n,\Upsilon_n) + a_2g(\psi_n,\Upsilon_n)\frac{h_2(\psi_{n+1},\psi_n)}{r_{n+1}} + \mathcal{O}(r^2),
\end{aligned}$$

Substitute into the update formula:

$$\begin{aligned}
\Upsilon_{n+1} &= \Upsilon_n + (b_1 + b_2(a_1+a_2))r^1_{n+1}\Xi(\psi_n,\Upsilon_n) \\
&+ a_1b_2(r^1_{n+1})^2\Delta_1\Xi(\psi_n,\Upsilon_n) + a_2b_2g(\psi_n,\Upsilon_n)h_2(\psi_{n+1},\psi_n) + \mathcal{O}(r^3).
\end{aligned}$$

Having established the general update formula, we now present our proof demonstrating the reduction to the classical method for the continuous case.

When $\mathbb{T} = \mathbb{R}$.

$$\begin{aligned}
&\sigma(\psi) = \psi, \quad \mu(\psi) = 0, \quad \Delta_1\Xi(\psi,\Upsilon) = \frac{\partial\Xi}{\partial\psi}(\psi,\Upsilon), \quad g(\psi,\Upsilon(\psi)) = \frac{\partial\Xi}{\partial\psi} + \Xi(\psi,\Upsilon)\frac{\partial\Xi(\psi,\Upsilon)}{\partial\Upsilon}, \\
&\Upsilon_{n+1} = \Upsilon_n + (b_1 + b_2(a_1+a_2))r\Xi(\psi_n,\Upsilon_n) + r^2(a_1b_2 + \frac{1}{2}a_2b_2)\frac{\partial\Xi(\psi_n,\Upsilon_n)}{\partial\psi} \\
&\quad + \frac{1}{2}a_2b_2r^2\Xi(\psi_n,\Upsilon_n)\frac{\partial\Xi(\psi,\Upsilon)}{\partial\Upsilon} + \mathcal{O}(r^3), \\
&\Upsilon_{n+1} = \Upsilon_n + (a_1+a_2)r\Xi(\psi_n,\Upsilon_n) + r^2a_2p_1\frac{\partial\Xi(\psi_n,\Upsilon_n)}{\partial\psi} + a_2q_{11}r^2\Xi(\psi_n,\Upsilon_n)\frac{\partial\Xi(\psi,\Upsilon)}{\partial\Upsilon} + \mathcal{O}(r^3),
\end{aligned}$$

where,

$$k_1 = \Xi(\psi_n,\Upsilon_n),$$

Uncorrected Proof

$$
\begin{aligned}
k_2 &= \Xi(\psi_n, \Upsilon_n) + rp_1 \frac{\partial \Xi(\psi_n, \Upsilon_n)}{\partial \psi} + rq_{11}\Xi(\psi_n, \Upsilon_n)\frac{\partial \Xi(\psi_n, \Upsilon_n)}{\partial \Upsilon} + \mathcal{O}(r^2) \\
&= \Xi(\psi_n + p_1 r, \Upsilon_n + q_{11} r \Xi(\psi_n, \Upsilon_n)), \\
\Upsilon_{n+1} &= \Upsilon_n + r(a_1 k_1 + a_2 k_2).
\end{aligned}
$$

□

5. Examples

Example 5.1. Solve the initial value problem (IVP) associated with dynamic equation,

$$\Upsilon^{\Delta} = 2\Upsilon + \psi^2 \quad , \Upsilon(0) = 1 \quad , \quad \mathbb{T} = [0,1] \cup [3,4].$$

Solution The numerical results for this example are presented using two techniques, as shown below:
Where the exact solution is [8]:

$$\Upsilon(\psi) = \begin{cases} \frac{5}{4}e^{2\psi} - \frac{\psi^2}{2} - \frac{\psi}{2} - \frac{1}{4}, & 0 \le \psi \le 1, \\ 5e^{2\psi-4} - \frac{25}{4}e^{2\psi-8} + \frac{19}{2}e^{2\psi-6} - \frac{\psi^2}{2} - \frac{\psi}{2} - \frac{1}{4}, & 3 \le \psi \le 4. \end{cases}$$

To find Runge-Kutta formula

$$
\begin{aligned}
\Xi(\psi, \Upsilon) &= 2\Upsilon + \psi^2, \\
\Xi_{\Upsilon} &= 2, \\
\Delta_1 \Xi(\psi, \Upsilon) &= \Xi_{\psi}(\psi, \Upsilon) = 2\psi, \qquad which \;\; \psi \in \mathbb{R}, \\
h_2(\psi^1_{n+1}, \psi_n) &= \frac{(\psi^1_{n+1} - \psi_n)^2}{2}, \qquad which \;\; \psi \in \mathbb{R}, \\
g(\psi, \Upsilon) &= \Delta_1 \Xi(\psi, \Upsilon(\psi)) + \left(\int_0^1 \frac{\partial}{\partial \Upsilon} \Xi(\sigma(\psi), \Upsilon(\psi) + s\mu(\psi)\Xi(\psi, \Upsilon(\psi)))ds \right) \Xi(\psi, \Upsilon(\psi)) \\
&= 2\psi + \left(\int_0^1 2ds \right) (2\Upsilon + \psi^2) \\
&= 2\psi + 4\Upsilon + 2\psi^2.
\end{aligned}
$$

$$
\begin{aligned}
\Upsilon_n + \frac{h_2(\psi^1_{n+1}, \psi_n) g(\psi_n, \Upsilon_n)}{\Xi_{\Upsilon}(\psi_n, \Upsilon_n) r^1_{n+1}} &= \Upsilon_n \frac{\left(\psi^1_{n+1} - \psi_n\right)^2}{2} \cdot \frac{(2\psi_n + 4\Upsilon_n + 2\psi_n^2)}{2r} \\
&= \Upsilon_n + \frac{(r^2)(2\psi_n + 4\Upsilon_n + 2\psi_n^2)}{4r} \\
&= \Upsilon_n + \frac{1}{4} r \left(2\psi_n + 4\Upsilon_n + 2\psi_n^2\right) \\
&= \Upsilon_n + \frac{1}{2} r \left(\psi_n + 2\Upsilon_n + \psi_n^2\right), \\
k_1 &= \Xi(\psi_n, \Upsilon_n) \\
&= 2\Upsilon_n + \psi_n^2, \\
k_2 &= a_1 \Xi(\psi^1_{n+1}, \Upsilon_n) + a_2 \Xi(\psi_n, \Upsilon_n + \frac{h_2(\psi^1_{n+1}, \psi_n) g(\psi_n, \Upsilon_n)}{\Xi_{\Upsilon}(\psi_n, \Upsilon_n) r^1_{n+1}}), \\
&= a_1 \left(2\Upsilon_n + (\psi_n + r)^2\right) + a_2 \left(2\Upsilon_n + r\left(\psi_n + 2\Upsilon_n + \psi_n^2\right) + \psi_n^2\right), \\
\Upsilon_{n+1} &= \Upsilon_n + r(b_1 k_1 + b_2 k_2).
\end{aligned}
$$

Uncorrected Proof

TABLE 4. Comparison of exact and numerical solutions over time ψ.

ψ	Υ_{exact}	Υ_{Euler} [8]	Υ_{RK}	Euler Error [8]	RK Error
0	1	1	1	0	0
0.11111	1.2493	1.2493	1.2493	2.8468e-06	2.3121e-11
0.22222	1.5637	1.5637	1.5637	7.2653e-06	5.7752e-11
0.33333	1.9624	1.9624	1.9624	1.3861e-05	1.0819e-10
0.44444	2.4695	2.4695	2.4695	2.3445e-05	1.8017e-10
0.55556	3.1151	3.1151	3.1151	3.7096e-05	2.8126e-10
0.66667	3.9366	3.9365	3.9366	5.6243e-05	4.2152e-10
0.77778	4.9808	4.9807	4.9808	8.2777e-05	6.1418e-10
0.88889	6.3064	6.3063	6.3064	0.00011919	8.7655e-10
1	7.9863	7.9862	7.9863	0.00016875	1.2315e-09
3.1111	50.302	50.301	50.302	0.00012592	8.4378e-10
3.2222	64.065	64.065	64.065	0.00031467	2.1073e-09
3.3333	81.343	81.342	81.343	0.00058971	3.9485e-09
3.4444	103.01	103.01	103.01	0.00098231	6.5745e-09
3.5556	130.17	130.17	130.17	0.001534	1.0262e-08
3.6667	164.18	164.18	164.18	0.0022995	1.5378e-08
3.7778	206.76	206.76	206.76	0.0033512	2.2405e-08
3.8889	260.04	260.04	260.04	0.004784	3.1978e-08
4	326.69	326.68	326.69	0.0067226	4.4928e-08

At P = 2:

$$\begin{cases} a_1 = b_1 = 0, \\ a_2 = 2, \quad b_2 = 1. \end{cases}$$

$$a_1 = 0, \quad a_2 = 2, \quad b_1 = 0, \quad b_2 = 0.5.$$

Euler method: We know the Euler method formula takes the form:

$$\Upsilon_{n+1} = \Upsilon_n + r(2\Upsilon_n + \psi_n^2), \quad n \in 1, ..., m.$$

The results of this method were shown in [8].

- Table 4 presents a side-by-side comparison of the exact analytical solution (Υ_{exact}) against numerical approximations obtained via the Euler method (Υ_{Euler}) and our proposed two-stage Runge-Kutta scheme (Υ_{RK}), evaluated over the hybrid time scale $\psi \in [0, 1] \cup [3, 4]$.
- The rightmost columns record the absolute truncation errors for each method, serving as a direct measure of numerical accuracy.
- As the table shows, Υ_{RK} tracks the exact solution far more closely than Υ_{Euler}: Runge-Kutta errors remain within the 10^{-11} to 10^{-8} band, whereas Euler errors reach the 6.7×10^{-3} level.
- The Euler method exhibits a clear pattern of error growth with increasing ψ, reaching a peak deviation of 0.0067; by contrast, the proposed scheme keeps its maximum error below 4.49×10^{-8} throughout the interval.
- Taken together, these results support the conclusion that the adapted Runge-Kutta formulation offers substantially better accuracy and stability for problems posed on hybrid or non-contiguous time domains.

Table 4 shows the exact solution (Υ_{Exact}) and the numerical solution by Euler method (Υ_{Euler}), Runge-Kutta method (Υ_{RK}) across different time points (ψ)and absolute errors. Comparison of absolute truncation errors among the Euler, and Runge-Kutta methods.

In Figure 1, displays two plots. The first compares the exact and numerical solutions, demonstrating a high level of accuracy. The second displays the absolute error, which remains strictly below 10^{-8} across the entire time interval.

In Figure 2, a logarithmic scale is used because the absolute errors are too small to be clearly distinguished on a standard linear axis. The Euler method exhibits the largest error across the interval; its error accumulates rapidly, reflecting lower accuracy and stability, and reaches a maximum of approximately 6.7×10^{-3}. In contrast, our proposed

Uncorrected Proof

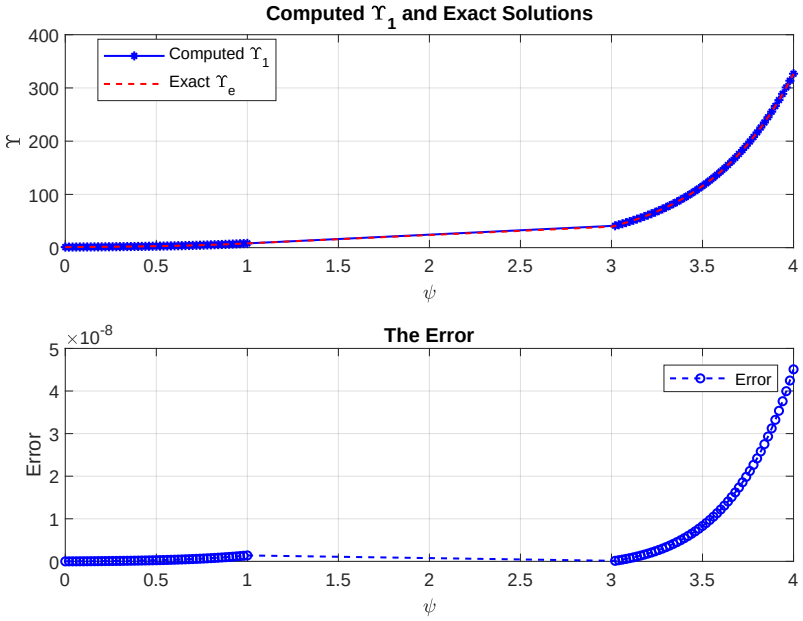


FIGURE 1. The first figure shows a comparison between the exact and numerical solutions. The second figure presents the absolute error, calculated as the difference between the numerical and exact solutions.

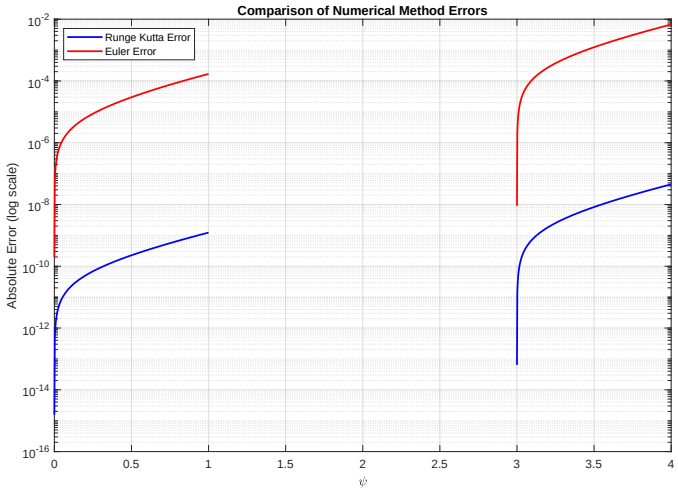


FIGURE 2. Absolute truncation error comparison across the hybrid time scale for Example 5.1.

second-stage Runge-Kutta method produces a substantially smaller error profile. Benefiting from its second-order formulation, it proves to be highly accurate and stable, restricting the maximum error to roughly 4.5×10^{-8}.

To confirm the theoretical second-order accuracy established in Theorem 4.1, we perform a convergence study for Example 5.1. The method is applied with five step sizes, each half of the previous one. The maximum absolute error

TABLE 5. Convergence study for Example 5.1: maximum absolute error $E(r)$ and computed convergence rate p under successive step-size halving on $\mathbb{T} = [0,1] \cup [3,4]$.

Step size r	**Max Error** $E(r)$	**Rate** p
1.60×10^{-4}	1.149801×10^{-5}	—
8.00×10^{-5}	2.874848×10^{-6}	1.9998
4.00×10^{-5}	7.187580×10^{-7}	1.9999
2.00×10^{-5}	1.796956×10^{-7}	2.0000
1.00×10^{-5}	4.492762×10^{-8}	1.9999

is defined as:

$$E(r) = \max_n |\Upsilon_{\text{exact}}(\psi_n) - \Upsilon_n|,$$

and the convergence rate is computed as [16, 22]:

$$p = \log_2\left(\frac{E(2r)}{E(r)}\right).$$

If the method is truly second-order accurate, the computed rate p should be close to 2.00 at every refinement level.

The computed rate $p \approx 2.00$ at every refinement level confirms that the proposed two-stage Runge-Kutta method achieves exactly second-order accuracy, consistent with the theoretical result established in Theorem 4.1. Specifically, each time the step size is halved, the maximum error reduces by a factor of approximately 4, which is the defining property of a second-order method [16, 19, 22].

Example 5.2. Solve the initial value problem (IVP) associated with dynamic equation,

$$\Upsilon^{\Delta} = 2\Upsilon + \sin_2(2\psi, \psi), \quad \Upsilon(0) = 1, \quad \mathbb{T} = [0, 0.5] \cup [2, 3] \cup [4, 4.5]. \tag{5.1}$$

Solution Where the exact solution is [8]:

$$\Upsilon(\psi) = \begin{cases} e^{2\psi}\left[\frac{5}{4} - \frac{1}{4}e^{-2\psi}\sin(2\psi) - \frac{1}{4}e^{-2\psi}\cos(2\psi)\right], & 0 \le \psi \le 0.5, \\ e^{2(\psi-2)}\left[4\left(e^1 + \frac{1}{4} - \frac{1}{4}e^{-1}\sin(1) - \frac{1}{4}e^{-1}\cos(1)\right) + \frac{3}{2}\sin(1)\right. \\ \quad \left. - \frac{1}{4}e^{4-2\psi}\sin(2\psi) - \frac{1}{4}e^{4-2\psi}\cos(2\psi) + \frac{1}{4}\sin(4) + \frac{1}{4}\cos(4)\right], & 2 \le \psi \le 3, \\ e^{2(\psi-4)}\left[e^3\left(1 + \frac{3}{2}\sin(1)\right)(1 + \sin(6))\right. \\ \quad + e^2\left(1 + \frac{3}{2}\sin(1)\right)(1 + \sin(6))\left(\frac{1}{4} - \frac{1}{4}e^{-1}\sin(1) - \frac{1}{4}e^{-1}\cos(1)\right) \\ \quad + e^2\left(\frac{3}{2}\sin(1)\right)(1 + \sin(6)) + \sin(6) \\ \quad + e^2(1 + \sin(6))\left(\frac{1}{4}\sin(4) + \frac{1}{4}\cos(4) - \frac{1}{4}e^{-2}\sin(6) - \frac{1}{4}e^{-2}\cos(6)\right) \\ \quad \left. - \frac{1}{4}e^{8-2\psi}\sin(2\psi) - \frac{1}{4}e^{8-2\psi}\cos(2\psi) + \frac{1}{4}\sin(8) + \frac{1}{4}\cos(8)\right], & 4 \le \psi \le 4.5. \end{cases} \tag{5.2}$$

Uncorrected Proof

To find Runge-Kutta formula

$$\Xi(\psi,\Upsilon)=2\Upsilon+\sin_2(2\psi,\psi),\quad \Xi_\Upsilon=2.$$

$$\Delta_1\Xi(\psi,\Upsilon)=\Xi_\psi(\psi,\Upsilon)=2\cos(2\psi),\quad h_2(\psi^1_{n+1},\psi_n)=\frac{(\psi_{n+1}-\psi_n)^2}{2}.$$

$$g(\psi,\Upsilon)=\Delta_1\Xi(\psi,\Upsilon(\psi))+\left(\int_0^1\frac{\partial}{\partial\Upsilon}\Xi(\sigma(\psi),\Upsilon(\psi)+s\mu(\psi)\Xi(\psi,\Upsilon(\psi)))ds\right)\Xi(\psi,\Upsilon(\psi)),$$
$$=2\cos(2\psi)+\left(\int_0^1 2ds\right)(2\Upsilon+\sin(2\psi))=2\cos(2\psi)+4\Upsilon+2\sin(2\psi).$$

$$\Upsilon_n+\frac{h_2(\psi^1_{n+1},\psi_n)g(\psi_n,\Upsilon_n)}{\Xi_\Upsilon(\psi_n,\Upsilon_n)r_{n+1}}=\Upsilon_n+\frac{\frac{(\psi^1_{n+1}-\psi_n)^2}{2}(2\cos(2\psi_n)+4\Upsilon_n+2\sin(2\psi_n))}{2r},$$
$$=\Upsilon_n+\frac{1}{2}r\left(\cos(2\psi_n)+2\Upsilon_n+\sin(2\psi_n)\right).$$

$$k_1=\Xi(\psi_n,\Upsilon_n)=2\Upsilon_n+\sin(2\psi_n).$$

$$k_2=a_1\Xi(\psi^1_{n+1},\Upsilon_n)+a_2\Xi(\psi_n,\Upsilon_n+\frac{h_2(\psi^1_{n+1},\psi_n)g(\psi_n,\Upsilon_n)}{\Xi_\Upsilon(\psi_n,\Upsilon_n)r_{n+1}}),$$
$$=a_1\left(2\Upsilon_n+\sin(2(\psi_n+r))\right)+a_2\left(2\Upsilon_n+r\left(\cos(2\psi_n)+2\Upsilon_n+\sin(2\psi_n)\right)+\sin(2\psi_n)\right).$$

$$\Upsilon_{n+1}=\Upsilon_n+r(b_1k_1+b_2k_2).$$

At P = 2:

$$\begin{cases}a_1=b_1=0,\\ a_2=2,\quad b_2=1.\end{cases}$$

$$a_1=0,\quad a_2=2,\quad b_1=0,\quad b_2=0.5.$$

Table 6 presents a comparison of the exact solution (Υ_{exact}) and the numerical solution ($\Upsilon_{\text{Numerical}}$) at selected time points (ψ), with the absolute error, defined as $|\Upsilon_{\text{exact}}-\Upsilon_{\text{Numerical}}|$, shown in the last column. The numerical solution agrees closely with the exact solution throughout the time domain, with errors remaining well below 10^{-6} across the entire interval. Notably, the accuracy is maintained even as ψ increases, confirming that the proposed method is stable and reliable over extended time spans.

Figure 3 presents two plots. The upper panel compares the exact solution (Υ_e, dashed red line) and the numerical solution (Υ_1, solid blue line) over the time variable ψ. The two curves are virtually indistinguishable throughout the interval, demonstrating a high level of numerical accuracy. The lower panel plots the absolute error between Υ_e and Υ_1 over the same domain. The error remains uniformly small throughout, confirming the stability and precision of the proposed method.

Example 5.3. Solve the initial value problem (IVP) associated with dynamic equation,

$$\Upsilon^\Delta=3\Upsilon+e_3(2\psi,\psi),\quad \Upsilon(0)=1,\quad \mathbb{T}=[0,1]\cup[3,3.75]\cup[4,4.25].$$

Solution Where the exact solution is [8]:

$$\Upsilon(\psi)=\begin{cases}e^{3\psi}\left[1+\psi\right], & 0\le\psi\le1,\\ e^{3(\psi-3)}\left[9e^3-3e^9+\psi e^9+7\right], & 3\le\psi\le3.75,\\ e^{3(\psi-4)}[\frac{63}{4}e^{\frac{21}{4}}+\frac{49}{4}e^{\frac{9}{4}}+\frac{25}{16}e^{\frac{45}{4}}+e^{12}(\psi-4)], & 4\le\psi\le4.25.\end{cases}$$

Uncorrected Proof

TABLE 6. Comparison between analytical and numerical solutions for ψ.

ψ	Υ_{exact}	$\Upsilon_{\text{Numerical}}$	Error
0.07142	1.15888890895502	1.15888896236761	5.34125885742753 e-08
0.28377	1.85970675994458	1.85970771764912	9.57704540116566 e-07
0.34235	2.12720862368934	2.12721006382349	1.44013414571376e-06
2.2844	21.9615820585416	21.9615786621409	3.39640070379232 e-06
2.34352	24.6555817683904	24.6555773205984	4.4477920511099 e-06
2.81088	62.0891718417798	62.089153548861	1.82929187531045 e-05
2.81145	62.1596437974134	62.1596254801235	1.83172899212991 e-05
2.85741	68.1164297241355	68.1164093652348	2.03589006559923 e-05
2.98619	88.0638861518313	88.0638591798929	2.69719384533573 e-05
4.0154	279.800073726814	279.800073880597	1.53783105361072 e-07
4.08439	321.268943827364	321.268944718182	8.90817602794414 e-07
4.1982	403.504110491904	403.504112766508	2.27460475343833 e-06
4.33146	526.859157801737	526.859161955333	4.15359545513638 e-06
4.36791	566.726904336522	566.726909052398	4.71587577521859 e-06
4.41895	627.66624025221	627.666245790893	5.53868301267357 e-06

Red Proof

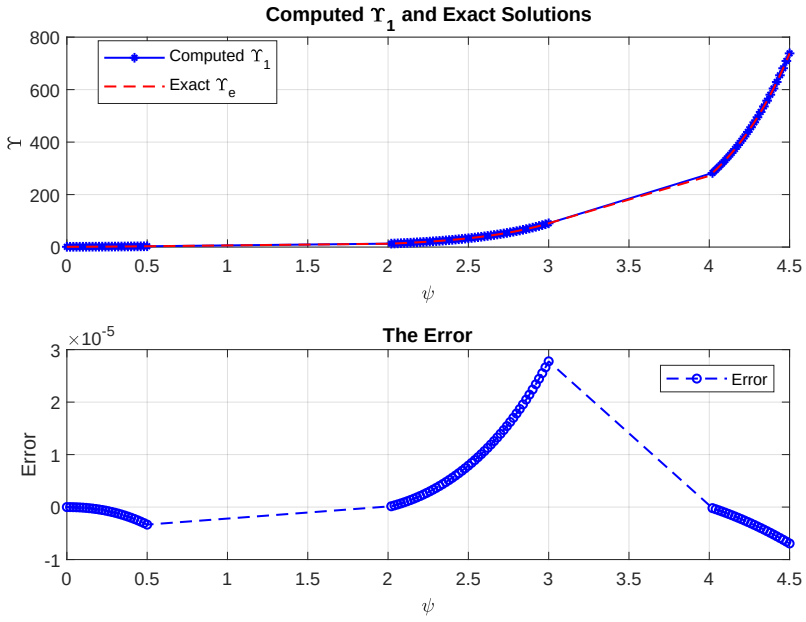


FIGURE 3. The first figure shows a comparison between the exact and numerical solutions. The second figure presents the corresponding error, calculated as the difference between the numerical and exact solutions.

To find Runge-Kutta formula

$$\Xi(\psi,\Upsilon) = 3\Upsilon + e_3(2\psi,\psi).$$

$$\Xi_\Upsilon = 3.$$

$$\Delta_1\Xi(\psi,\Upsilon) = \Xi_\psi(\psi,\Upsilon) = 3e^{3\psi}.$$

$$h_2(\psi^1_{n+1},\psi_n) = \frac{(\psi^1_{n+1}-\psi_n)^2}{2}.$$

$$g(\psi,\Upsilon) = \Delta_1\Xi(\psi,\Upsilon(\psi)) + \left(\int_0^1 \frac{\partial}{\partial\Upsilon}\Xi(\sigma(\psi),\Upsilon(\psi)+s\mu(\psi)\Xi(\psi,\Upsilon(\psi))ds\right)\Xi(\psi,\Upsilon(\psi)) = 6e^{3\psi}+9\Upsilon.$$

$$\Upsilon_n + \frac{h_2(\psi^1_{n+1},\psi_n)g(\psi_n,\Upsilon_n)}{\Xi_\Upsilon(\psi_n,\Upsilon_n)r^1_{n+1}} = \Upsilon_n + \frac{1}{2}r\left(2e^{3\psi_n}+3\Upsilon_n\right).$$

$$k_1 = \Xi(\psi_n,\Upsilon_n) = 3\Upsilon_n + e^{3\psi_n}.$$

$$k_2 = a_1\Xi(\psi^1_{n+1},\Upsilon_n) + a_2\Xi(\psi_n,\Upsilon_n + \frac{h_2(\psi^1_{n+1},\psi_n)g(\psi_n,\Upsilon_n)}{\Xi_\Upsilon(\psi_n,\Upsilon_n)r_{n+1}}),$$
$$= a_1\left(3\Upsilon_n + e^{3(\psi_n+r)}\right) + a_2\left(3\Upsilon_n + 3re^{3\psi_n} + \frac{9}{2}r\Upsilon_n + e^{3\psi_n}\right).$$

$$\Upsilon_{n+1} = \Upsilon_n + r(b_1k_1 + b_2k_2).$$

At P = 2:

$$\begin{cases} a_1 = b_1 = 0, \\ a_2 = 2, \quad b_2 = 1. \end{cases}$$

$a_1 = 0, \quad a_2 = 2, \quad b_1 = 0, \quad b_2 = 0.5.$

- The table show each of the exact solution (Υ_e) and the numerical solution (Υ_1) across different time points (ψ).
- The absolute error is defined as the difference between the exact and numerical solution it is included in last column.
- Results show that the numerical solution is very close to the exact solution, with very small errors throughout the time range.
- the error so small that mean the method perform well even as ψ increases, The error remains uniformly small across the entire time domain. This suggests it's a dependable approach for solving dynamic problems over longer time spans.

Figure 4 displays two plots. The first compares the exact and numerical solutions, demonstrating a high level of accuracy. The second displays the absolute error, which remains strictly below 10^{-5} across the entire time interval.

Example 5.4. Solve the initial value problem (IVP) associated with dynamic equation, when $\mathbb{T} = \mathbb{N}_0$:

$$\Upsilon^\Delta(\psi) = \frac{1}{\psi+1}\Upsilon(\psi) + \frac{1}{\psi^2+1}, \quad \Upsilon(0) = 1.$$

Solution The exact solution:

$$\Upsilon(\psi_n) = (\psi_{n+1})\left(\Upsilon_0 + \sum_{p=0}^{\psi_n-1}\frac{1}{(p+2)(p^2+1)}\right).$$

Uncorrected Proof

TABLE 7. Temporal Comparison of Analytical and Computational Solutions for ψ.

ψ	Υ_{exact}	$\Upsilon_{\text{Numerical}}$	Error
0.06366	1.28749155071228	1.28749155064184	7.04454272693056 e-11
0.09234	1.4410070135884	1.44100701347624	1.12155618126053 e-10
0.19426	2.13893223029971	2.13893222997139	3.28323146447929 e-10
0.37372	4.21513824165923	4.21513824053083	1.12839515509222 e-09
0.55384	8.18455864165715	8.18455863866825	2.98890334704538 e-09
0.63418	10.9537421801376	10.9537421757054	4.43213465928238 e-09
0.76308	17.3970783218489	17.3970783137798	8.06912936468507 e-09
0.87745	26.108592459121	26.1085924457304	1.33906183918953 e-08
0.89111	27.3986559224257	27.398655908218	1.42076430620364 e-08
0.97947	37.3838626779348	37.3838626572105	2.07242578653677 e-08
3.29252	6152.25399800509	6152.2539950052	2.99988460028544 e-06
3.38962	10764.9428536644	10764.9428480955	5.56883969693445 e-06
3.4121	12143.111221278	12143.1112149188	6.35926699033007 e-06
3.41861	12567.7930503047	12567.7930437001	6.60457408230286 e-06
3.50924	19878.2916905377	19878.2916796053	1.09324028016999 e-05
3.53095	22081.1758244564	22081.1758121874	1.22689598356374 e-05
3.59031	29211.7611188597	29211.7611021847	1.66750214702915 e-05
3.64688	37806.6765690776	37806.6765469602	2.21173686441034 e-05
4.15037	231922.024583536	231922.024551852	3.16842342726886 e-05

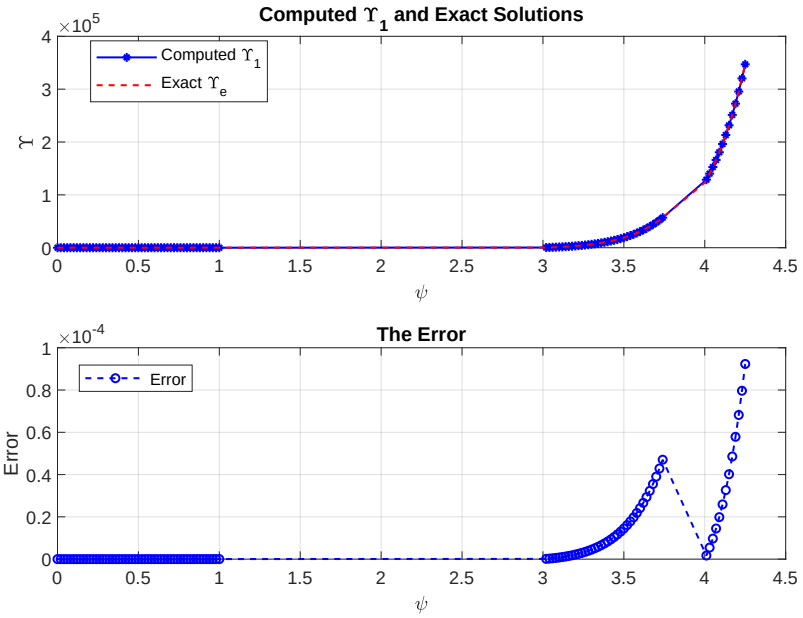


FIGURE 4. The first figure shows a comparison between the exact and numerical solutions. The second figure presents the absolute error, calculated as the difference between the numerical and exact solutions.

A Proof

To find Runge-Kutta formula:

$$\Xi(\psi,\Upsilon)=\frac{\Upsilon}{\psi+1}+\frac{1}{\psi^2+1},$$

$$\Xi_{\Upsilon}(\psi,\Upsilon)=\frac{1}{\psi+1},$$

$$\Delta_1\Xi(\psi,\Upsilon)=\Xi(\psi+1,\Upsilon)-\Xi(\psi,\Upsilon)=\frac{\Upsilon\psi^2+2\Upsilon\psi+2\Upsilon+\psi+2}{(\psi+2)(\psi^2+2\psi+2)}-\frac{\Upsilon\psi^2+\Upsilon+\psi+1}{(\psi+1)(\psi^2+1)},$$

$$\Xi(\sigma(\psi),\Upsilon+S\mu(\psi)\Xi(\psi,\Upsilon))=\frac{\Upsilon\psi^3+\Upsilon\psi^2+\Upsilon\psi+\Upsilon+S(\Upsilon\psi^2+\Upsilon+\psi+1)}{(\psi+2)(\psi+1)(\psi^2+1)}+\frac{1}{(\psi+1)^2+1},$$

$$\frac{\partial}{\partial\Upsilon}\Xi(\sigma(\psi),\Upsilon+s\mu(\psi)\Xi(\psi,\Upsilon))=\frac{\psi^3+\psi^2+\psi+1+s\psi^2+s}{(\psi+2)(\psi+1)(\psi^2+1)},$$

$$g(\psi,\Upsilon)=\Delta_1(\psi,\Upsilon)+\left(\int_0^1\frac{\partial}{\partial\Upsilon}\Xi(\sigma(\Upsilon),\Upsilon+s\mu(\psi)\Xi(\psi,\Upsilon))ds\right)\Xi(\psi,\Upsilon)$$

$$=\frac{\Upsilon\psi^2+2\Upsilon\psi+2\Upsilon+\psi+2}{(\psi+2)(\psi^2+2\psi+2)}-\frac{\Upsilon\psi^2+\Upsilon+\psi+1}{(\psi+1)(\psi^2+1)}+\left(\frac{3+2\psi}{2(\psi+1)(\psi+2)}\right)\left(\frac{\Upsilon}{\psi+1}+\frac{1}{\psi^2+1}\right),$$

$$h_2(\psi^1_{n+1},\psi_n)=\frac{r(r-1)}{2},$$

$$\Upsilon_n+\frac{\Delta_1\Xi(\psi_n,\Upsilon_n)}{\Xi_{\Upsilon}(\psi_n,\Upsilon_n)}r^1_{n+1}=\Upsilon_n+r(1+\psi_n)\left(\frac{2+\psi_n+2\Upsilon_n+2\psi_nx_n+\psi_n^2\Upsilon_n}{(\psi_n+2)(\psi_n^2+2\psi_n+2)}-\frac{1+\psi_n+\Upsilon_n+\psi_n^2\Upsilon_n}{(\psi_n+1)(\psi_n^2+1)}\right),$$

$$\Upsilon_n+\frac{h_2(\psi^1_{n+1},\psi_n)g(\psi_n,\Upsilon_n)}{\Xi_{\Upsilon}(\psi_n,\Upsilon_n)r^1_{n+1}}=\Upsilon_n+\frac{1}{2}(r-1)(\psi_n+1)\left[\frac{\Upsilon_nt_n^2+2\Upsilon_nt_n+2\Upsilon_n+\psi_n+2}{(\psi_n+2)(\psi_n^2+2\psi_n+2)}\right.$$

$$\left.-\frac{\Upsilon_n\psi_n^2+\Upsilon_n+\psi_n+1}{(\psi_n+1)(\psi_n^2+1)}+\frac{3+2\psi_n}{2(\psi_n+1)(\psi_n+2)}\left(\frac{\Upsilon_n}{\psi_n+1}+\frac{1}{\psi_n^2+1}\right)\right],$$

$$k_1=\Xi(\psi_n,\Upsilon_n)=\frac{\Upsilon_n}{\psi_n+1}+\frac{1}{\psi_n^2+1},$$

$$k_2=a_1\Xi(\psi^1_{n+1},\Upsilon_n)+a_2\Xi\left(\psi_n,\Upsilon_n+\frac{h_2(\psi^1_{n+1},\psi_n)g(\psi_n,\Upsilon_n)}{\Xi_{\Upsilon}(\Upsilon_n,\psi_n)r^1_{n+1}}\right)$$

$$=a_1\left(\frac{\Upsilon_n}{\psi_n+r+1}+\frac{1}{(\psi_n+1)^2+1}\right)$$

$$+a_2\left[\frac{1}{\psi_n^2+1}+\frac{\Upsilon_n+\frac{1}{2}(r-1)(1+\psi_n)}{\psi_n+1}\times\left[\frac{\Upsilon_n\psi_n^2+2\Upsilon_n\psi_n+2\Upsilon_n+\psi_n+2}{(\psi_n+2)(\psi_n^2+2\psi_n+2)}\right.\right.$$

$$\left.\left.-\frac{\Upsilon_n\psi_n^2+\Upsilon_n+\psi_n+1}{(\psi_n+1)(\psi_n^2+1)}+\frac{3+2\psi_n}{2(\psi_n+1)(\psi_n+2)}\times\left(\frac{\Upsilon_n}{\psi_n+1}+\frac{1}{\psi_n^2+1}\right)\right]\right].$$

$$\Upsilon_{n+1}=\Upsilon_n+r(b_1k_1+b_2k_2).$$

At P = 2:

$$\begin{cases}a_1=b_1=0,\\ a_2=2,\quad b_2=1.\end{cases}$$

$$a_1=0,\quad a_2=2,\quad b_1=0,\quad b_2=0.5.$$

- Table 8 presents the integer-valued time points $\psi\in\mathbb{N}_0$, the exact solution

$$\Upsilon_{exact}(\psi)=(\psi+1)\left(\Upsilon_0+\sum_{p=0}^{\psi-1}\frac{1}{(p+2)(p^2+1)}\right),$$

Uncorrected Proof

TABLE 8. Pointwise comparison of the exact solution Υ_{exact}, the Runge-Kutta approximation $\Upsilon_{Numercical}$, and the absolute error at integer nodes $\psi \in \mathbb{N}_0$ for the rational dynamic equation in Example 5.4.

ψ	Υ_{exact}	$\Upsilon_{\text{Numerical}}$	Error
0	1.00000	1.00000	0.00000
1	3.00000	3.00000	0.00000
2	5.00000	5.00000	0.00000
4	8.68333333333333	8.68333333333333	0.00000
5	10.4788235294118	10.4788235294118	1.77635683940025e-15
6	12.2637556561086	12.2637556561086	1.77635683940025e-15
7	14.0427477768654	14.0427477768654	1.77635683940025e-15
8	15.8180912489736	15.8180912489736	3.5527136788005e-15
10	19.3623408365087	19.3623408365087	0.00000
12	22.9016892370654	22.9016892370654	3.5527136788005e-15
13	24.6702541916407	24.6702541916407	3.5527136788005e-15
14	26.4382975582705	26.4382975582705	3.5527136788005e-15
15	28.2059268709538	28.2059268709538	3.5527136788005e-15
16	29.9732220791495	29.9732220791495	3.5527136788005e-15
17	31.7402438402714	31.7402438402714	7.105427357601e-15
18	33.5070389961485	33.5070389961485	0.00000
19	35.2736442874438	35.2736442874438	7.105427357601e-15
20	37.0400889327552	37.0400889327552	7.105427357601e-15

its Runge-Kutta counterpart $\Upsilon_{Numerical}$, and the absolute deviation between them.

- Since the underlying time scale is $\mathbb{T} = \mathbb{N}_0$, the graininess satisfies $\mu(\psi) = 1$ at every node, collapsing the general time-scale formula to its purely discrete form. Under these conditions, floating-point round-off is the sole remaining source of discrepancy.

- Across the full range $\psi = 0, 1, \ldots, 20$, the observed errors do not exceed $\sim 10^{-15}$, a magnitude consistent with double-precision machine epsilon. This indicates that the second-stage scheme recovers the exact solution to the limit of representable arithmetic on integer time scales.

- Crucially, the deviation neither grows nor exhibits any recognisable trend as ψ increases. This flat error profile reflects genuine long-term stability and confirms that the method is well suited to rational-type equations over extended discrete domains.

Example 5.4 ($\mathbb{T} = \mathbb{N}_0$). Upper panel: the exact solution Υ_e (dashed red) plotted alongside the Runge-Kutta approximation $\Upsilon_{Numerical}$ (solid blue) at successive integer nodes; the two sequences overlap completely at the scale of the figure. Lower panel: absolute error remaining at the level of machine epsilon throughout, indicating thatno numerical degradation occurs as the solution grows with ψ, see Figure 5.

Example 5.5. Solve the initial value problem (IVP) associated with dynamic equation, when $\mathbb{T} = \mathbb{N}_0$, this equation represents a simple population growth model and on an arbitrary time scale:

$$\Upsilon^{\Delta}(\psi) = (\alpha \ominus (\alpha\Upsilon(\psi)))\Upsilon(\psi), \quad \Upsilon(0) = 2, \quad \psi > 0.$$

$$\Upsilon^{\Delta}(\psi) = \frac{\alpha(1-\Upsilon)}{1+\alpha\mu(\psi)\Upsilon}\Upsilon, \quad \alpha = 2, \quad \mathbb{T} = \mathbb{N}_0.$$

Uncorrected Proof

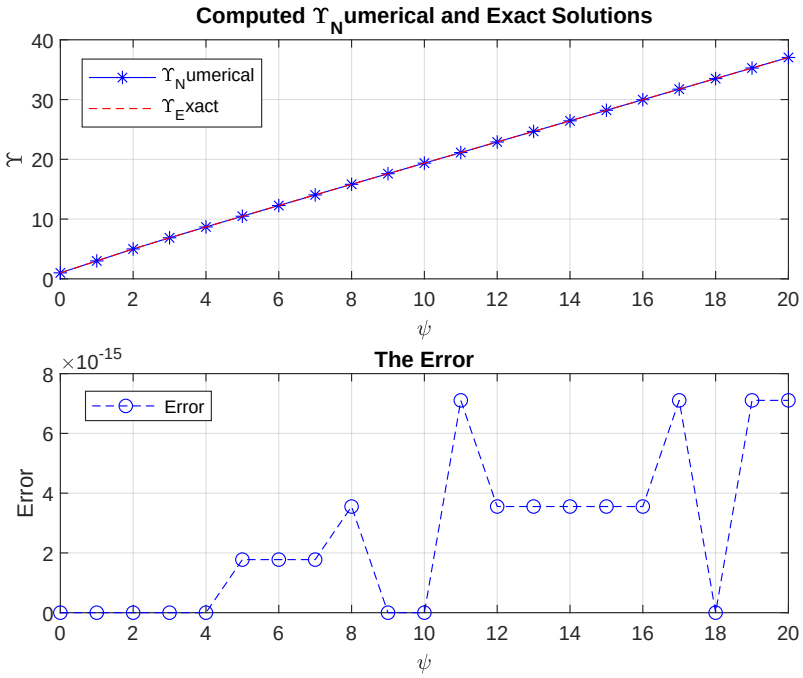


FIGURE 5. The first figure shows a comparison between the exact and numerical solutions. The second figure presents the absolute error, calculated as the difference between the numerical and exact solutions.

Uncorrected

Solution The exact solution is:

$$\Upsilon_i(\psi) = \frac{(1+\alpha)\Upsilon_{i-1}(\psi)}{1+\alpha\Upsilon_{i-1}(\psi)}, \quad \alpha = 2, \quad i \in \{1,2,3,4,\dots\}.$$

To find Runge-Kutta formula

$$\sigma(\psi) = \psi + 1, \quad \mu(\psi) = 1, \quad \Xi(\psi_n, \Upsilon_n) = \frac{\alpha(1-\Upsilon_n)}{1+\alpha\Upsilon_n}\Upsilon_n.$$

$$\Xi_\Upsilon = \frac{\alpha - \Upsilon(\alpha+\alpha^2) - \alpha^2\Upsilon^2}{(1+\alpha\Upsilon)^2}, \quad \Delta_1\Xi(\psi, X) = \Xi(\psi+1, \Upsilon) - \Xi(\psi, \Upsilon) = 0.$$

$$h_2(\psi^1_{n+1}, \psi_n) = \frac{(\psi^1_{n-1} - \psi_n)(\psi^1_{n+1} - \psi_n - 1)}{2} = \frac{r(r-1)}{2}.$$

$$\begin{aligned} g(\psi, \Upsilon) &= \Delta_1\Xi(\psi, \Upsilon(\psi)) + \left(\int_0^1 \frac{\partial}{\partial\Upsilon}\Xi(\sigma(\psi), \Upsilon(\psi) + s\mu(\psi)\Xi(\psi, \Upsilon(\psi)))\, ds\right)\Xi(\psi, \Upsilon(\psi)), \\ &= 0 + \left[\int_0^1 \frac{\partial}{\partial\Upsilon}\Xi\left(\psi+1, \Upsilon + \frac{s\alpha\Upsilon(1-\Upsilon)}{1+\alpha\Upsilon}\right) ds\right]\Xi(\psi, \Upsilon) \\ &= \frac{\alpha^2\Upsilon(1-\Upsilon)}{(1+\Upsilon\alpha)^3}\left[\frac{1}{2} - \Upsilon - \frac{\Upsilon^2\alpha}{2} + \frac{-7 - \Upsilon(-15+\alpha) + \alpha + 8\Upsilon^2\alpha}{(-1+\Upsilon)\alpha}\right. \\ &\quad \left. - \frac{(1+\Upsilon\alpha)^2\left(1+\alpha+8\Upsilon^2\alpha(2+\alpha) - \Upsilon(2+11\alpha+\alpha^2)\right)}{(-1+\Upsilon)^2\Upsilon^2\alpha^4}\right. \end{aligned}$$

$$
\begin{aligned}
&- \frac{(1+\Upsilon\alpha)^2\left(1+\alpha+8\Upsilon^3\alpha^2+\Upsilon^2\alpha(31+7\alpha)-2\Upsilon(1+9\alpha)\right)\ln\left[(1+\Upsilon\alpha)^2\right]}{(-1+\Upsilon)^2\Upsilon^2\alpha^4}\\
&+ \frac{(1+\Upsilon\alpha)^2\left(1+\alpha+8\Upsilon^2\alpha(2+\alpha)-\Upsilon(2+11\alpha+\alpha^2)\right)}{(1+\Upsilon\alpha(2+\alpha))(-1+\Upsilon)^2\Upsilon^2\alpha^4}\\
&+ \frac{(1+\Upsilon\alpha)^2\left(1+\alpha+8\Upsilon^3\alpha^2+\Upsilon^2\alpha(31+7\alpha)-2\Upsilon(1+9\alpha)\right)\ln\left[1+\Upsilon\alpha(2+\alpha)\right]}{(-1+\Upsilon)^2\Upsilon^2\alpha^4}\Bigg].
\end{aligned}
$$

$$
\begin{aligned}
\Upsilon_n + \frac{h_2(\psi^1_{n+1},\psi_n)g(\psi_n,\Upsilon_n)}{\Xi_\Upsilon(\psi_n,\Upsilon_n)r^1_{n+1}} &= \Upsilon_n + \frac{(r-1)}{2}\cdot\frac{(1+\alpha\Upsilon_n)^2}{\alpha-\Upsilon_n(\alpha+\alpha^2)-\alpha^2\Upsilon_n^2}\\
&+ \frac{\alpha^3\Upsilon_n(1-\Upsilon_n)}{(1+\alpha\Upsilon_n)^3}\left(\frac{1}{2}-\Upsilon_n-\frac{\Upsilon_n^2\alpha}{2}+\frac{-7-\Upsilon_n(-15+\alpha)+\alpha+8\Upsilon_n^2\alpha}{(-1+\Upsilon_n)\alpha}\right.\\
&\left.- \frac{(1+\alpha\Upsilon_n)^2\left(1+\alpha+8\Upsilon_n^2\alpha(2+\alpha)-\Upsilon_n(2+11\alpha+\alpha^2)\right)}{(-1+\Upsilon_n)^2}\right)\\
&+ \frac{(1+\alpha\Upsilon_n)^2}{(-1+\Upsilon_n)^2\Upsilon_n^2\alpha^4}\left(1+\alpha+8\Upsilon_n^3\alpha^2+\Upsilon_n^2\alpha(31+7\alpha)\right.\\
&\left.- 2\Upsilon_n(1+9\alpha)\log[(1+\alpha\Upsilon_n)^2]\right)\\
&+ \frac{(1+\alpha\Upsilon_n)^2}{(-1+\Upsilon_n)^2\Upsilon_n^2\alpha^4}\left(\frac{(1+\alpha\Upsilon_n)^2\left(1+\alpha+8\Upsilon_n^2\alpha(2+\alpha)-\Upsilon_n(2+11\alpha+\alpha^2)\right)}{1+\Upsilon_n\alpha(2+\alpha)}\right.\\
&\left.+\left(1+\alpha+8\Upsilon_n^3\alpha^2+\Upsilon_n^2\alpha(31+7\alpha)-2\Upsilon_n(1+9\alpha)\right)\log[1+\Upsilon_n\alpha(2+\alpha)]\right).
\end{aligned}
$$

$$
k_1 = \Xi(\psi_n,\Upsilon_n) = \frac{\alpha(1-\Upsilon_n)}{1+\alpha\Upsilon_n}\Upsilon_n,
$$

$$
\begin{aligned}
k_2 &= a_1\Xi(\psi^1_{n+1},\Upsilon_n) + a_2\Xi\left(\psi_n,\Upsilon_n+\frac{h_2(\psi^1_{n+1},\psi_n)g(\psi_n,\Upsilon_n)}{\Xi_\Upsilon(\Upsilon_n,\psi_n)r^1_{n+1}}\right)\\
&= a_1\frac{\alpha(1-\Upsilon_n)}{1+\alpha\Upsilon_n}\Upsilon_n + a_2\frac{\alpha\left(\Upsilon_n-\frac{(r-1)(1-\Upsilon_n)\Upsilon_n\alpha^2E}{2(\alpha\Upsilon_n+1)D}\right)\left(-\Upsilon_n+\frac{(r-1)(1-\Upsilon_n)\Upsilon_n\alpha^2E}{2(\alpha\Upsilon_n+1)D}+1\right)}{\alpha\Upsilon_n-\frac{(r-1)(1-\Upsilon_n)\Upsilon_n\alpha^3E}{2(\alpha\Upsilon_n+1)D}+1},
\end{aligned}
$$

where

$$
\begin{aligned}
&A=\alpha\Upsilon_n,\quad B=1-\Upsilon_n,\quad C=A+1,\quad D=\alpha\Upsilon_n^2+(\alpha+1)\Upsilon_n-1,\\
&E=-\frac{A\Upsilon_n}{2}-\Upsilon_n+\frac{8\alpha\Upsilon_n^2-(\alpha-15)\Upsilon_n+\alpha-7}{(\Upsilon_n-1)\alpha}+\frac{C^2\cdot F}{(\Upsilon_n-1)^2\Upsilon_n^2\alpha^4},\\
&F=\frac{(8\alpha(\alpha+2)\Upsilon_n^2-(\alpha^2+11\alpha+2)\Upsilon_n+\alpha+1)C^2}{\Upsilon_n\alpha(\alpha+2)+1}\\
&\quad+\left(8\alpha^2\Upsilon_n^3+\alpha(7\alpha+31)\Upsilon_n^2-2(9\alpha+1)\Upsilon_n+\alpha+1\right)\log(\Upsilon_n\alpha(\alpha+2)+1)\\
&\quad+\frac{1}{2}-\frac{C^2(8\alpha(\alpha+2)\Upsilon_n^2-(\alpha^2+11\alpha+2)\Upsilon_n+\alpha+1)}{(\Upsilon_n-1)^2\Upsilon_n^2\alpha^4}\\
&\quad-\frac{C^2\left(8\alpha^2\Upsilon_n^3+\alpha(7\alpha+31)\Upsilon_n^2-2(9\alpha+1)\Upsilon_n+\alpha+1\right)\log(C^2)}{(\Upsilon_n-1)^2\Upsilon_n^2\alpha^4}.
\end{aligned}
$$

$$
\Upsilon_{n+1} = \Upsilon_n + r(b_1k_1+b_2k_2).
$$

Uncorrected Proof

TABLE 9. Reference solution Υ_{exact} obtained from the exact recurrence, Runge-Kutta approximation $\Upsilon_{Numerical}$, and absolute error for Example 5.5.

ψ	Υ_{exact}	$\Upsilon_{\text{Numerical}}$	Error
0	2.00000	2 .00000	0.00000
2	1.05882352941176	1.05882352942002	8.25961521400131e-12
3	1.0188679245283	1.01886792453212	3.81539244642681e-12
5	1.0020618556701	1.00206185567079	6.82343070934621e-13
6	1.00068634179822	1.00068634179849	2.71338507218388e-13
9	1.00002540327702	1.00002540327704	1.44328993201270e-14
10	1.0000084676156	1.00000846761561	5.10702591327572e-15
13	1.00000031361284	1.00000031361284	2.22044604925031e-16
15	1.00000003484586	1.00000003484586	4.44089209850063e-16
16	1.00000001161529	1.00000001161529	0.00000
18	1.00000000129059	1.00000000129059	2.22044604925031e-16
19	1.0000000004302	1.0000000004302	4.44089209850063e-16
21	1.0000000000478	1.0000000000478	0.00000
22	1.00000000001593	1.00000000001593	0.00000
23	1.00000000000531	1.00000000000531	2.22044604925031e-16
24	1.00000000000177	1.00000000000177	2.22044604925031e-16
26	1.0000000000002	1.0000000000002	2.22044604925031e-16
27	1.00000000000007	1.00000000000007	2.22044604925031e-16
28	1.00000000000002	1.00000000000002	0.00000
30	1.00000	1.00000	6.66133814775094e-16

The method is consistent of order $p = 2$ if

$$\begin{cases} a_1 = b_1 = 0, \\ a_2 b_2 = 1. \end{cases}$$

$a_1 = 0, \quad a_2 = 2, \quad b_1 = 0, \quad b_2 = 0.5.$

- Table 9 tabulates the discrete time index ψ, the reference solution generated by the exact recurrence

$$\Upsilon_i = \frac{(1+\alpha)\Upsilon_{i-1}}{1+\alpha\Upsilon_{i-1}},$$

with $\alpha = 2$, the corresponding Runge-Kutta value Υ_1, and their absolute difference, for the nonlinear logistic population model.
- A distinguishing feature of this example is that the right-hand side carries no explicit dependence on ψ, making $\Delta_1 \Xi = 0$ identically. The second-stage correction therefore originates entirely from the nonlinear Υ-structure through $g(\psi, \Upsilon)$, yet second-order accuracy is preserved throughout.
- The recorded errors fall in the range 0 to 7.1×10^{-15}, well within the bounds of floating-point arithmetic. This confirms that the scheme accurately tracks the logistic saturation towards the carrying capacity $\Upsilon \to 1$ without introducing spurious oscillations or drift.
- Near the equilibrium $\Upsilon = 1$ the error shows no sign of amplification, which is a non-trivial property for nonlinear recurrences. The result establishes that the adapted method remains well-conditioned even as the solution approaches a stable fixed point.

Figure 6 presents two panels. The upper panel compares the exact solution Υ_e (dashed red) with the numerical approximation Υ_N (solid blue) at successive integer nodes; the two sequences overlap completely. The lower panel shows the absolute error, which remains at the level of machine epsilon throughout, confirming that no numerical degradation occurs as the solution approaches the carrying capacity.

Uncorrected Proof

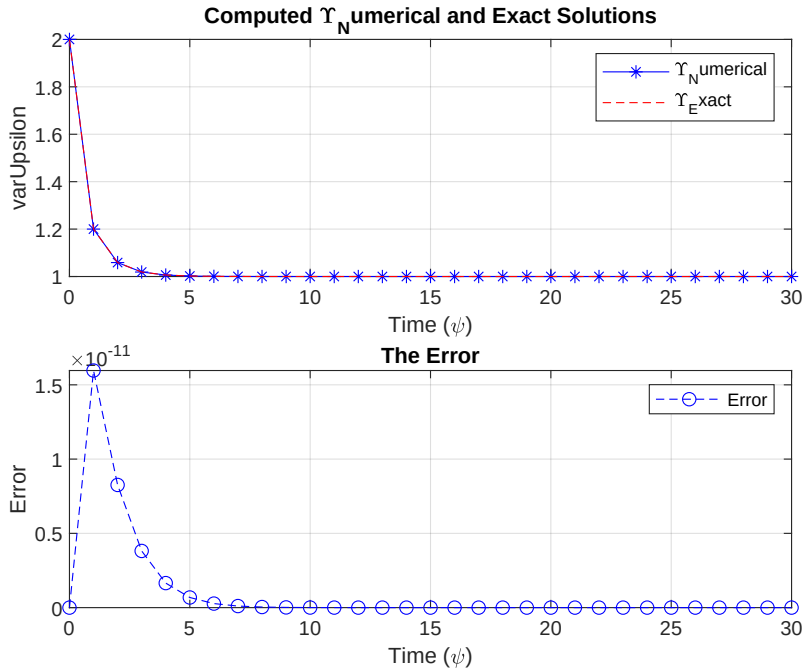


FIGURE 6. The first figure shows a comparison between the exact and numerical solutions. The second figure presents the absolute error, calculated as the difference between the numerical and exact solutions.

Example 5.6. Our example is an initial value problem associated with a Riccati-type dynamic equation:

$$\Upsilon^{\Delta} = [\ominus(-\psi)]\Upsilon^{\sigma} + \frac{\Upsilon^2}{\mu(\psi)\Upsilon - \frac{1}{\psi}}, \quad \Upsilon(2) = 1.5, \tag{5.6}$$

on the time scale $\mathbb{T} = \{2, 4, 6\} \cup [7, 8]$.

Solution The equation can be written as:

$$\Upsilon^{\Delta} = \frac{\psi}{1 - \mu(\psi)\psi}\Upsilon(\sigma(\psi)) + \frac{\Upsilon^2(\psi)\psi}{\mu(\psi)\psi\Upsilon - 1}. \tag{5.3}$$

To apply the explicit Runge-Kutta method, we express $\Upsilon^{\Delta}(\psi)$ purely as a function of ψ and $\Upsilon(\psi)$. We utilize the fundamental time scale property $\Upsilon(\sigma(\psi)) = \Upsilon(\psi) + \mu(\psi)\Upsilon^{\Delta}(\psi)$ and substitute it into Equation (5.6):

$$\Upsilon^{\Delta}(\psi) = \frac{\psi}{1 - 2\mu(\psi)\psi}\Upsilon(\psi) + \frac{(1 - \mu(\psi)\psi)\psi\Upsilon^2(\psi)}{(1 - 2\mu(\psi)\psi)(\mu(\psi)\psi\Upsilon(\psi) - 1)} = \Xi(\psi, \Upsilon).$$

For a second-order Runge-Kutta approximation, the update formula is:

$$\Upsilon_{n+1} = \Upsilon_n + r(b_1k_1 + b_2k_2),$$

Where r is the step size, and the stage approximations are:

$$k_1 = \Xi(\psi_n, \Upsilon_n),$$

$$k_2 = a_1\Xi(\psi_{n+1}, \Upsilon_n) + a_2\Xi\left(\psi_n, \Upsilon_n + \frac{h_2(\psi_{n+1}, \psi_n)g(\psi_n, \Upsilon_n)}{\Xi_{\Upsilon}(\Upsilon_n, \psi_n)r_{n+1}^1}\right).$$

Uncorrected

The partial derivative of the explicit function with respect to Υ, denoted as $\Xi_\Upsilon(\psi, \Upsilon)$:

$$\Xi_\Upsilon(\psi, \Upsilon) = \frac{\psi}{1 - 2\mu(\psi)\psi} + \frac{(1 - \mu(\psi)\psi)(\mu(\psi)\psi\Upsilon^2 - 2\Upsilon)}{(1 - 2\mu(\psi)\psi)(\mu(\psi)\psi\Upsilon - 1)^2},$$

The partial derivative of the explicit function with respect to ψ, denoted as Δ_1, Δ_1 takes two forms:

For the isolated discrete points where the graininess function $\mu(\psi) > 0$, it is defined as:

$$\Delta_1\Xi(\psi_n, \Upsilon_n) = \frac{\Xi(\sigma(\psi_n), \Upsilon_n) - \Xi(\psi_n, \Upsilon_n)}{\mu(\psi_n)},$$

For the continuous interval where $\mu(\psi) = 0$, it reduces to the classical partial derivative with respect to time:

$$\Delta_1\Xi(\psi_n, \Upsilon_n) = \frac{\partial\Xi(\psi_n, \Upsilon_n)}{\partial\psi}.$$

To calculate the function $g(\psi, \Upsilon)$:

This operator Δ_1 is inserted directly as the leading term to formulate the auxiliary function $g(\psi_n, \Upsilon_n)$, which tracks the second-order dynamics of the system:

$$g(\psi_n, \Upsilon_n) = \Delta_1\Xi(\psi_n, \Upsilon_n) + \left(\int_0^1 \frac{\partial\Xi}{\partial\Upsilon}\Big(\sigma(\psi_n), \Upsilon_n + s\mu(\psi_n)\Xi(\psi_n, \Upsilon_n)\Big)\, ds\right)\Xi(\psi_n, \Upsilon_n).$$

Apply Runge-Kutta to the Discrete Domain $\mathbb{T} = \{2, 4, 6\}$ For isolated points where the graininess function $\mu(\psi) > 0$, the time-scale monomial $h_2 = 0$.

Step 1: From $\psi_0 = 2$ to $\psi_1 = 4$

Here, we initialize the first discrete step.

- $\Upsilon_0 = 1.5$, $\sigma(2) = 4 \implies \mu(2) = 2$. The step size is $r = 2$.
- Calculate K_1: Substituting the initial values into the explicit equation $\Xi(\psi, \Upsilon)$:

$$k_1 = \Xi(2, 1.5) = \frac{2(1.5)}{1 - 2(2)(2)} + \frac{(1 - 2(2))(2)(1.5)^2}{(1 - 2(2)(2))(2(2)(1.5) - 1)}$$

$$k_1 = \frac{3}{1 - 8} + \frac{(-3)(2)(2.25)}{(-7)(4(1.5) - 1)}$$

$$k_1 = -\frac{3}{7} + \frac{-13.5}{-7(5)} = -\frac{3}{7} + \frac{13.5}{35} = \frac{-15 + 13.5}{35} = -\frac{1.5}{35} = -\frac{3}{70}.$$

- Calculate Partial Derivative Ξ_Υ:

$$\Xi_\Upsilon(2, 1.5) = \frac{2}{1 - 8} + \frac{(1 - 4)(4(1.5)^2 - 2(1.5))}{(1 - 8)(4(1.5) - 1)^2},$$

$$\Xi_\Upsilon(2, 1.5) = -\frac{2}{7} + \frac{(-3)(9 - 3)}{(-7)(25)} = -\frac{2}{7} + \frac{-18}{-175} = \frac{-50 + 18}{175} = -\frac{32}{175}.$$

- Calculate Auxiliary Function Δ_1:

$$\Delta_1\Xi(2, 1.5) = \frac{\Xi(4, 1.5) - \Xi(2, 1.5)}{\mu(2)} = \frac{\Xi(4, 1.5) - (-3/70)}{2},$$

We then substitute Δ_1 as the leading term to formulate the auxiliary function g:

$$g(2, 1.5) = \Delta_1\Xi(2, 1.5) + \left(\int_0^1 \frac{\partial\Xi}{\partial\Upsilon}\Big(4, 1.5 + s(2)(-3/70)\Big)ds\right)\Xi(2, 1.5).$$

.

- Calculate k_2 and Update Υ_1:

$$k_2 = 2\Xi\left(2, 1.5 + \frac{2}{2}\frac{g(2, 1.5)}{-32/175}\right).$$

$$\Upsilon_1 = 1.5 + 2(0.5K_2) = 1.5 + k_2.$$

Uncorrected Proof

Step 2: From $\psi_1 = 4$ to $\psi_2 = 6$ We proceed with the newly calculated Υ_1.
$\sigma(4) = 6 \implies \mu(4) = 2$. The step size is $r = 2$.

$$k_1 = \Xi(4, \Upsilon_1).$$
$$\Xi_\Upsilon(4, \Upsilon_1) = \frac{4}{1-16} + \frac{(1-8)(8\Upsilon_1^2 - 2\Upsilon_1)}{(1-16)(8\Upsilon_1 - 1)^2}.$$

Just like the first step, we formulate the discrete first-order finite difference operator (Δ_1):

$$\Delta_1 \Xi(4, \Upsilon_1) = \frac{\Xi(6, \Upsilon_1) - \Xi(4, \Upsilon_1)}{\mu(4)}.$$

We then substitute Δ_1 as the leading term to formulate the auxiliary function g:

$$g(4, \Upsilon_1) = \Delta_1 \Xi(4, \Upsilon_1) + \left(\int_0^1 \frac{\partial \Xi}{\partial \Upsilon} \Big(6, \Upsilon_1 + s(2)(-0.015)\Big)\, ds \right) \Xi(4, \Upsilon_1),$$
$$g(4, \Upsilon_1) = \frac{\Xi(6, \Upsilon_1 + 2k_1) - \Xi(4, \Upsilon_1)}{2},$$
$$k_2 = 2\Xi \left(4, \Upsilon_1 + \frac{2}{2} \frac{g(4, \Upsilon_1)}{\Xi_\Upsilon(4, \Upsilon_1)} \right),$$
$$\Upsilon_2 = \Upsilon_1 + k_2.$$

Step 3: From $\psi_2 = 6$ to $\psi_3 = 7$ This is the final discrete step before entering the continuous domain.

- $\sigma(6) = 7 \implies \mu(6) = 1$. The step size is $r = 1$.
- Calculate K_1:

$$k_1 = \Xi(6, \Upsilon_2) = \frac{6}{1 - 2(1)(6)} \Upsilon_2 + \frac{(1 - 1(6))(6)\Upsilon_2^2}{(1 - 2(1)(6))(1(6)\Upsilon_2 - 1)},$$
$$k_1 = -\frac{6}{11} \Upsilon_2 + \frac{30\Upsilon_2^2}{11(6\Upsilon_2 - 1)}.$$

- Calculate Δ_1 and g:

$$\Delta_1 \Xi(6, \Upsilon_2) = \frac{\Xi(7, \Upsilon_2) - \Xi(6, \Upsilon_2)}{1}.$$
$$g(6, \Upsilon_2) = \Delta_1 \Xi(6, \Upsilon_2) + \left(\int_0^1 \frac{\partial \Xi}{\partial \Upsilon} \Big(7, \Upsilon_2 + sK_1\Big) ds \right) \Xi(6, \Upsilon_2).$$

- Calculate k_2 and Update Υ_3: With $h_2(7, 6) = 0$:

$$k_2 = 2\Xi \left(6, \Upsilon_2 + \frac{1}{2} \frac{g(6, \Upsilon_2)}{\Xi_\Upsilon(6, \Upsilon_2)} \cdot (\mathbf{0}) \right) = 2\Xi(6, \Upsilon_2) = 2k_1.$$

Update the state variable as it enters the continuous domain:

$$\Upsilon_3 = \Upsilon_2 + \frac{r}{2}(K_2) = \Upsilon_2 + k_1.$$

Step 4: Evaluating the Continuous Domain (From $\psi = 7$ to $\psi = 8$)
At $\psi = 7$, the system enters the continuous interval. The graininess function drops to zero ($\mu(\psi) = 0$), meaning the time-scale equations naturally reduce to their continuous forms. This demonstrates the unified power of the method, as we use the exact same algebraic formula derived for the discrete points.

The explicit function and its partial derivative reduce to:

$$\Xi(\psi, \Upsilon) = \psi\Upsilon - \psi\Upsilon^2.$$
$$\Xi_\Upsilon(\psi, \Upsilon) = \psi - 2\psi\Upsilon.$$

Uncorrected Proof

Because the domain is continuous, Δ_1 simplifies to the partial time derivative. The unified auxiliary function $g(\psi, \Upsilon)$ is evaluated as:

$$g(\psi,\Upsilon) = \frac{\partial \Xi}{\partial \psi} + \left(\int_0^1 \Xi_\Upsilon(\psi,\Upsilon)ds\right)\Xi(\psi,\Upsilon),$$
$$g(\psi,\Upsilon) = (\Upsilon - \Upsilon^2) + (\psi - 2\psi\Upsilon)(\psi\Upsilon - \psi\Upsilon^2),$$
$$g(\psi,\Upsilon) = \Upsilon(1-\Upsilon)\left[1 + \psi^2 - 2\psi^2\Upsilon\right].$$

For the continuous step size r, the second-order time-scale monomial evaluates to $h_2(\psi + r, \psi) = \frac{r^2}{2}$. We now apply the exact same unified Runge-Kutta formula used in the previous steps:

$$k_1 = \Xi(\psi_n, \Upsilon_n).$$
$$k_2 = 2\Xi\left(\psi_n, \Upsilon_n + \frac{r}{2}\frac{g(\psi_n,\Upsilon_n)}{\Xi_\Upsilon(\psi_n,\Upsilon_n)}\right),$$
$$k_2 = 2\Xi\left(\psi_n, \Upsilon_n + \frac{r}{2}\frac{\Upsilon_n(1-\Upsilon_n)[1+\psi_n^2 - 2\psi_n^2\Upsilon_n]}{\psi_n(1-2\Upsilon_n)}\right).$$

Finally, the state variable is updated:

$$\Upsilon_{n+1} = \Upsilon_n + \frac{r}{2}k_2.$$

This confirms that a single, unified mathematical framework successfully governs both the scattered points and the continuous intervals. To maintain an acceptable residual error bound, a step size $r = 0.0001$ is used.

The method is consistent of order $p = 2$ if

$$\begin{cases} a_1 = b_1 = 0, \\ a_2 b_2 = 1. \end{cases}$$

$a_1 = 0, \quad a_2 = 2, \quad b_1 = 0, \quad b_2 = 0.5.$

- Table 10 reports the computed values $\Upsilon_{\text{Numerical}}$ together with the substitution residual $|\text{LHS} - \text{RHS}|$ at selected points of the hybrid domain $\mathbb{T} = \{2, 4, 6\} \cup [7, 8]$. Given the absence of a closed-form analytical solution for this Riccati-type problem on a mixed time scale, back-substitution into the original dynamic equation serves as the primary validation criterion.
- At each of the three isolated points $\psi \in \{2, 4, 6\}$ the residual is exactly zero, consistent with the fact that $h_2 = 0$ holds at those nodes and the discrete step is executed without truncation. A brief residual peak appears near $\psi = 7$, precisely where the graininess transitions abruptly from $\mu > 0$ to $\mu = 0$; beyond that point the residual decays steadily, reaching $\mathcal{O}(10^{-7})$ at $\psi = 8$.
- Throughout this transition the algorithm applies a single formula without any domain-specific branching. The absence of instability at the discrete-to-continuous interface is a direct consequence of how Δ_1 and h_2 are defined on the respective sub-domains, and it demonstrates the structural coherence of the time-scale framework.
- Taken together, the near-zero discrete residuals and the rapid post-transition decay confirm second-order consistency of the adapted scheme for Riccati-type problems on genuinely hybrid time scales, without requiring separate treatment of the continuous and scattered-point sub-domains.

Figure 7 above visually confirms the stability of our proposed approach for the Riccati-type equation. The top graph shows the numerical trajectory of Υ as it evolves across the hybrid time scale, stepping through the isolated discrete points ($\psi = 2, 4, 6$) before transitioning smoothly into the continuous interval $[7, 8]$. Since an exact analytical solution is difficult to pin down for this mixed domain, the bottom graph evaluates the method's fidelity by plotting the substitution residual error. This error represents the absolute difference between the numerical approximation (LHS) and the evaluated dynamic equation (RHS). As the plot demonstrates, the residual error remains exceptionally near to zero across the entire domain, proving that the numerical solution satisfies the original dynamic equation with a high degree of precision.

Uncorrected Proof

TABLE 10. Numerical solution $\Upsilon_{\text{Numerical}}$ and substitution residual error |LHS − RHS| Example 5.6.

ψ	$\Upsilon_{Numerical}$	Error
2.0000	1.50000000	0.00000
4.0000	1.41428571	0.00000
6.0000	1.38398892	0.00000
7.0000	1.34430148	1.11022302e-16
7.0996	1.14535813	5.33769769e-04
7.1996	1.06619603	2.03778142e-04
7.2996	1.03100337	8.89122072e-05
7.3996	1.01463079	4.11189617e-05
7.4996	1.00689304	1.94549157e-05
7.5996	1.00322814	9.25740965e-06
7.6996	1.00149964	4.39347015e-06
7.7996	1.00069036	2.07125141e-06
7.8996	1.00031478	9.68108445e-07
7.9996	1.00014213	4.48209974e-07
8.0000	1.00014168	4.46823005e-07

Proof

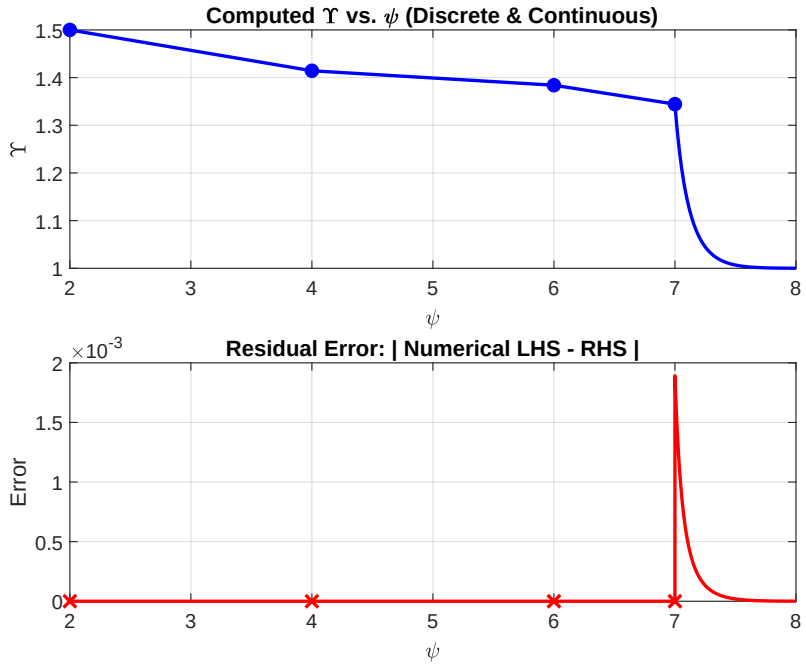


FIGURE 7. The top figure display we computed numerical solution Υ evaluated over the hybrid time domain $\mathbb{T} = \{2, 4, 6\} \cup [7, 8]$. The bottom figure presents the substitution residual error, calculated as the absolute difference between the numerical left-hand side (LHS) approximation and the evaluated right-hand side (RHS) of the dynamic equation.

TABLE 11. Stability test for Example 5.1 with $\varepsilon = 10^{-3}$: original solution Υ_{orig},perturbed solution Υ_{pert}, absolute difference, and relative difference over $\mathbb{T} = [0,1] \cup [3,4]$.

ψ	Υ_{orig}	Υ_{pert}	Abs. Diff	Rel. Diff
0.00000	1.0000000000	1.0010000000	1.000×10^{-3}	1.000×10^{-3}
0.11111	1.2493299012	1.2505787473	1.249×10^{-3}	9.996×10^{-4}
0.22222	1.5637198432	1.5652794598	1.560×10^{-3}	9.974×10^{-4}
0.33334	1.9624722359	1.9644199959	1.948×10^{-3}	9.925×10^{-4}
0.44445	2.4695727003	2.4720051528	2.432×10^{-3}	9.850×10^{-4}
0.55556	3.1150950175	3.1181327763	3.038×10^{-3}	9.752×10^{-4}
0.66667	3.9365570375	3.9403507307	3.794×10^{-3}	9.637×10^{-4}
0.77778	4.9808127805	4.9855505194	4.738×10^{-3}	9.512×10^{-4}
0.88889	6.3063757067	6.3122924134	5.917×10^{-3}	9.382×10^{-4}
3.00000	39.3494349744	39.3504349744	1.000×10^{-3}	2.541×10^{-5}
3.11111	50.3016185297	50.3028673758	1.249×10^{-3}	2.483×10^{-5}
3.22222	64.0651733183	64.0667329349	1.560×10^{-3}	2.434×10^{-5}
3.33333	81.3427702023	81.3447179234	1.948×10^{-3}	2.394×10^{-5}
3.44444	103.0119369430	103.0143693468	2.432×10^{-3}	2.361×10^{-5}
3.55555	130.1685706573	130.1716083554	3.038×10^{-3}	2.334×10^{-5}
3.66667	164.1846962829	164.1884899761	3.794×10^{-3}	2.311×10^{-5}
3.77778	206.7635167491	206.7682544880	4.738×10^{-3}	2.291×10^{-5}
3.88889	260.0423064546	260.0482231613	5.917×10^{-3}	2.275×10^{-5}
4.00000	326.6867830606	326.6941721167	7.389×10^{-3}	2.262×10^{-5}

5.1. **Stability Test Under Perturbed Initial Condition.** To verify the numerical stability of the proposed method, we solve Example 5.1 twice: once with the original initial condition $\Upsilon(0) = 1$, and once with a perturbed initial condition $\Upsilon(0) = 1 + \varepsilon$, where $\varepsilon = 10^{-3}$. A stable numerical method should produce solutions that remain proportionally close when the initial data are slightly changed [22].

Since the exact solution grows exponentially as $e^{2\psi}$, the absolute difference between the two solutions is expected to grow in the same manner. Therefore, the correct stability measure is the *relative difference*, defined as:

$$\delta_{\text{rel}}(\psi_n) = \frac{|\Upsilon_n^{\varepsilon} - \Upsilon_n|}{|\Upsilon_n|}.$$

If the method is stable, this relative difference should remain bounded and proportional to ε throughout the domain see Table 11.

The results confirm that the maximum relative difference remains bounded by $\varepsilon = 10^{-3}$ throughout the entire domain $\mathbb{T} = [0,1] \cup [3,4]$. The absolute difference grows proportionally to $e^{2\psi}$, which is an inherent property of the equation itself and not a deficiency of the method. This confirms that the proposed method is stable with respect to perturbations in the initial condition, in agreement with the stability theory of one-step methods [19, 22].

6. CONCLUSION

The two-stage Runge-Kutta method developed in this paper provides a single unified numerical scheme for dynamic equations on time scales, working without modification across continuous, discrete, and hybrid domains. The method is built on the delta derivative, the graininess function μ, the forward jump operator σ, and the time-scale monomial h_2. Theorem 4.1 established second-order consistency through a Taylor expansion argument on a general time scale $\mathbb{T}$, and the explicit reduction to the classical Runge-Kutta method when $\mathbb{T} = \mathbb{R}$ confirms the framework is a genuine generalization of the continuous case.

Six test problems validated the method across a wide range of settings. In all cases where an exact solution was available (Examples 5.1–5.5), the absolute errors fell between 10^{-8} and 10^{-15}. For Example 5.6, where no closed-form

Uncorrected Proof

analytical solution exists on the hybrid domain $\mathbb{T} = \{2, 4, 6\} \cup [7, 8]$, validation was instead performed through back-substitution into the original dynamic equation. The substitution residuals were exactly zero at the three isolated discrete nodes, reached a peak of approximately 5×10^{-4} immediately after the graininess transition at $\psi = 7$, and then decayed steadily to $\mathcal{O}(10^{-7})$ by $\psi = 8$. This peak is a direct consequence of the abrupt change in graininess at the discrete-to-continuous interface and not a sign of instability, since the residual decays monotonically beyond that point without any domain-specific adjustment to the formula.

Table 5 confirmed the theoretical rate $p \approx 2.00$ at every refinement level, and the stability test in Section 4.7 showed the relative error remained bounded by the perturbation size $\varepsilon = 10^{-3}$ throughout the domain with no amplification.

Three directions for future work follow naturally. First, an adaptive step-size mechanism based on a local error estimator would improve efficiency for problems with sharp gradients near domain transition points. Second, deriving third- and fourth-order variants using the s-stage framework of Definition 3.2 would extend applicability to problems demanding higher precision. Third, an implicit formulation incorporating the nabla derivative alongside the delta derivative would make the method suitable for stiff systems arising in control theory and population dynamics on time scales.

Ethics approval and consent to participate

The author confirm that all the results they obtained are new and there is no conflict of interest with anyone.

Consent for publication

All authors agree to publish.

Availability of data and materials

The data used to support the findings of this study are available from the corresponding author upon request.

Competing interests

There is no conflict of interest between the authors or anyone else regarding this manuscript.

Authors' Contribution

We confirm that the final authorship list is correct and that all individuals who have made significant contributions to this work have been included. All authors have given their permission to be named and have approved the final version of the manuscript.

Below is the detailed Authors' Contributions statement, which we have now included in the revised manuscript file (in the "Authors' Contribution" section): Khalid K. Ali- Conceptualization, methodology, formal analysis, writing - original draft, validation. K. R. Raslan– Formal analysis, investigation, writing - review & editing, validation. Mohamed S.Mohamed - Supervision, project administration, resources, writing - review & editing. Ahmed Azab - Software, numerical implementation, visualization, writing – review & editing.

Funding

The authors would like to acknowledge the Deanship of Graduate Studies and Scientific Research, Taif University for funding this work.

Acknowledgment

The authors would like to acknowledge the Deanship of Graduate Studies and Scientific Research, Taif University for funding this work.

Use of AI tools declaration

The authors declare they have not used Artificial Intelligence (AI) tools in the creation of this article.

Uncorrected Proof

References

[1] R. P. Agarwal and M. Bohner, *Basic calculus on time scales and some of its applications*, Results Math., *35*(1-2) (1999), 3–22.

[2] R. P. Agarwal, M. Bohner, D. O'Regan, and A. Peterson, *Dynamic equations on time scales: A survey*, J. Comput. Appl. Math., *141*(1-2) (2002), 1–26.

[3] P. Amster, C. Rogers, and C. C. Tisdell, *Existence of solutions to boundary value problems for dynamic systems on time scales*, J. Math. Anal. Appl., *308*(2) (2005), 565–577.

[4] F. M. Atici and G. S. Guseinov, *On Green's functions and positive solutions for boundary value problems on time scales*, J. Comput. Appl. Math., *141*(1-2) (2002), 75–99.

[5] F. M. Atici, D. C. Biles, and A. Lebedinsky, *An application of time scales to economics*, Math. Comput. Model., *43*(7-8) (2006), 718–726.

[6] F. M. Atici and F. Uysal, *A production-inventory model of HMMS on time scales*, Appl. Math. Lett., *21*(3) (2008), 236–243.

[7] B. Aulbach and S. Hilger, *Linear dynamic processes with inhomogeneous time scale*, In Nonlinear Dynamics and Quantum Dynamical Systems, Akademie Verlag, 1990, pp. 9–20.

[8] A. Azaba, K. R. Raslan, and K. K. Ali, *Solution of non-homogeneous dynamic equation on time scale*, Comput. Methods Differ. Equ., (2025).

[9] Z. Bartosiewicz and E. Pawłuszewicz, *Realizations of linear control systems on time scales*, Control Cybern., *35*(4) (2006), 1071–1086.

[10] M. Bohner and A. Peterson, *Dynamic Equations on Time Scales: An Introduction with Applications*, Birkhäuser, 2001.

[11] M. Bohner and A. Peterson, *Advances in Dynamic Equations on Time Scales*, Birkhäuser, Boston, 2003.

[12] M. Bohner, M. Fan, and J. Zhang, *Existence of periodic solutions in predator–prey and competition dynamic systems*, Nonlinear Anal. Real World Appl., *7*(5) (2006), 1193–1204.

[13] M. Bohner, M. Fan, and J. Zhang, *Periodicity of scalar dynamic equations and applications to population models*, J. Math. Anal. Appl., *330*(1) (2007), 1–9.

[14] M. Bohner and S. G. Georgiev, *Multivariable Dynamic Calculus on Time Scales*, Springer International Publishing, 2016.

[15] J. C. Butcher, *Numerical methods for ordinary differential equations in the 20th century*, J. Comput. Appl. Math., *125*(1-2) (2000), 1–29.

[16] J. C. Butcher, *Numerical Methods for Ordinary Differential Equations*, 2nd ed., John Wiley & Sons, Chichester, 2008.

[17] J. J. DaCunha, *Stability for time varying linear dynamic systems on time scales*, J. Comput. Appl. Math., *176*(2) (2005), 381–410.

[18] R. P. Feynman and A. R. Hibbs, *Quantum Mechanics and Path Integrals*, McGraw-Hill, 1965.

[19] S. G. Georgiev and İ. M. Erhan, *Numerical Analysis on Time Scales*, Walter de Gruyter GmbH, Berlin, 2022.

[20] G. S. Guseinov, *Integration on time scales*, J. Math. Anal. Appl., *285*(1) (2003), 107–127.

[21] M. Guzowska, A. B. Malinowska, and M. R. Sidi Ammi, *Calculus of variations on time scales: applications to economic models*, Adv. Differ. Equ., *2015* (2015), Article 203.

[22] E. Hairer, S. P. Nørsett, and G. Wanner, *Solving Ordinary Differential Equations I: Nonstiff Problems*, 2nd rev. ed., Springer-Verlag, Berlin, 1993.

[23] S. Hilger, *Ein Maßkettenkalkül mit Anwendung auf Zentrumsmannigfaltigkeiten*, PhD thesis, Universität Würzburg, 1988.

[24] S. Hilger, *Analysis on measure chains: A unified approach to continuous and discrete calculus*, Results Math., *18*(1-2) (1990), 18–56.

[25] S. Hilger, *Differential and difference calculus — unified!*, Nonlinear Anal., *30*(5) (1997), 2683–2694.

[26] J. Hoffacker and C. C. Tisdell, *Stability and instability for dynamic equations on time scales*, Comput. Math. Appl., *49*(9-10) (2005), 1327–1334.

Uncorrected Proof

[27] V. Lakshmikantham, S. Sivasundaram, and B. Kaymakcalan, *Dynamic Systems on Measure Chains*, Mathematics and its Applications, Vol. 370, Kluwer Academic Publishers, Dordrecht, 1996.
[28] W. N. Li, *Some new dynamic inequalities on time scales*, J. Math. Anal. Appl., *319*(2) (2006), 802–814.
[29] A. A. Martynyuk, *Stability Theory for Dynamic Equations on Time Scales*, Springer, 2016.
[30] A. O. Okech, J. O. Abonyo, and D. Theuri, *Taylor method and second-order Runge-Kutta method for solving a two-dimensional first order dynamic equations on time scales*, Glob. J. Pure Appl. Math., *14*(9) (2018), 1217–1236.
[31] A. C. Peterson and C. C. Tisdell, *Boundedness and uniqueness of solutions to dynamic equations on time scales*, J. Differ. Equ. Appl., *10*(13-15) (2004), 1295–1306.
[32] C. Pötzsche, *Chain rule and invariance principle on measure chains*, J. Comput. Appl. Math., *141*(1-2) (2002), 249–254.
[33] Y. H. Su and Z. Feng, *Variational approach for a p-Laplacian boundary value problem on time scales*, Appl. Anal., *97*(11) (2018), 1957–1971.
[34] J. Zhang, M. Fan, and H. Zhu, *Periodic solution of single population models on time scales*, Math. Comput. Model., *52*(3-4) (2010), 515–521.

Uncorrected Proof